the other hand, recent works also have progressively revealed the biological profile of HLA-E. Although the endogenous expression of HLA-E is confirmed in the vast range of cells and tissues,[4] the degree of cell surface expression is dependent on the availability of nonamer peptide derived from other HLA class I signal sequences.[5–8] In case of EVTs, the cell surface expression of HLA-E is implied to be supported by the supply of leader peptides of HLA-G and -C. Uterine natural killer (uNK) cells possibly respond to HLA-E on EVTs mediated by the inhibitory receptor, CD94/NKG2A. This immunological interaction could induce significant modulation in fetomaternal immunological paradigm.

Progesterone has been considered to be an essential hormone in maintaining pregnancy although its function is not fully elucidated. Among its fundamental roles, the action as an immunomodulator has been reported. Progesterone reduces the cytotoxic activity of NK cells[9] and T-cells,[10] and also modulates T helper 1 and T helper 2 balance.[11,12] Recently, progesterone has been reported to enhance the expression of HLA-G on trophoblasts.[13] Given that, HLA-G has specialized immunological function at the interface between mother and fetus, progesterone might contribute to the maternal immunological tolerance to the fetus through the regulation of HLA-G expression on trophoblasts. However, the influence of progesterone on HLA-E, another HLA class Ib molecule that affects the immune interaction between mother and fetus, has not been elucidated. In this study, we tried to investigate the effect of progesterone on HLA-E expression in trophoblasts at mRNA and protein level by using JEG-3 choriocarcinoma cell line.

Materials and methods

Cell Lines and Cultures

Human choriocarcinoma cell line JEG-3, was obtained from American Type Culture Collection (ATCC, Rockville, MD, USA) and maintained in RPMI 1640 (Sigma, St Louis, MO, USA) supplemented with 10% heat-inactivated fetal bovine serum (FBS) and antibiotics/antimycotics (GibcoBRL, Grand Island, NY, USA) at 37°C in a humidified 5% CO_2 atmosphere. Cells were seeded at a concentration of 1×10^5/mL. When cells were grown to approximately 60% confluence, we replaced media with serum-free RPMI1640. After 24 hr, the culture media were refreshed again and progesterone (10, 100, 1000 ng/mL) was added to the culture dishes assigned to each assay. In the case of inhibition assay, RU486 (1000 ng/mL) (Sigma) was concomitantly supplemented to the culture with progesterone. Progesterone and RU486 were dissolved into 99.5% ethanol and prepared in 10, 100 or 1000 μg/mL stock. 2 μL of the stock solution was added to 2 mL of culture media.

Reverse-transcriptase Reaction and Real-time Polymerase Chain Reaction

Total RNA of JEG-3 cells was extracted from the cells using RNAeasy Mini Kit (Qiagen, Hilden, Germany) and was reverse-transcribed with the ReverTraAce kit (Toyobo, Osaka, Japan) according to the manufacturer's instruction. Real-time polymerase chain reaction (PCR) was carried out using iCycler iQ Real-time PCR Detection System (Bio-Rad, Hercules, CA, USA). The sequences of gene-specific primers are summarized in Table I.[14] PCR was performed in a 20 μL volume containing aliquots of diluted cDNA, 0.5 μM primers, 2.3 mM $MgCl_2$ and 0.3 μL 100X SYBR Green I DNA master mixture (Roche Diagnostics, Lewes, UK). For negative control, water was used instead of the target cDNA template. After 3 min denaturation at 95°C, 40 cycles of amplification were carried out: 95°C denaturation for 20 s, 56°C annealing for 30 s, and 72°C extension for 30 s. Beta-actin was used as an internal control in each sample to compensate the variations in quantities and qualities among cDNA samples. The amount of HLA-E mRNA was normalized against that of beta-actin. The amplification specificity of PCR prod-

Table I Primers for Real-Time PCR of HLA-E

Primer	Forward primers	Reverse primers	Size
HLA-E	5′-GGGACACCGCACAGATTTT-3′	5′-CTCAGAGGCATCATTTGACTTTT-3′	254
Beta-actin	5′-AAGGCCAACCGCGAGAA-3′	5′-CCTCGTAGATGGGCACA-3′	166

ucts was confirmed by melting curve analysis and electrophoresis on a 2% agarose gel.

Flow Cytometric Analysis

Cultured JEG-3 cells were detached from culture plates with 0.05% trypsin-EDTA (GibcoBRL) after different culture periods. Cells were washed with PBS containing 1% FBS and 0.1% NaN_3 and incubated with saturating concentrations of anti-HLA-E-specific monoclonal antibody 3D12[5] (provided by Dr Daniel E Geraghty, Fred Hutchinson Cancer Research Center, Seattle, WA, USA), or mouse isotype-matched IgG1 (Dako, Glostrup, Denmark) for 30 min at 4°C. After washing three times to remove unbound antibody, the cells were incubated with fluorescein isothiocyanate-conjugated anti-mouse IgG $F(ab')_2$ rabbit IgG (Dako) for 30 min at 4°C. The cells were subsequently resuspended in PBS containing 1% paraformaldehyde for detection. Fifty thousand cells were detected for each sample using a Coulter EPICSR XL flow cytometer (Beckman Coulter, Tokyo, Japan) and the data analysis was carried out using EXPO32™ software (Beckman Coulter).

Statistics

Statistical analysis was carried out using Wilcoxon test for pair-matched samples. When P value was less than 0.05, the difference was regarded as statistically significant.

Results

Effect of Progesterone on HLA-E mRNA Expression

Human leukocyte antigen-E mRNA amount of JEG-3 cells treated with 1000 ng/mL of progesterone increased up to 3.5-fold of that of control ($P < 0.05$) at 1 hr culture, while no significant increase was observed at 30 min, 2, 3 and 4 hr (Fig. 1a). Addition of 10 or 100 ng/mL of progesterone did not show any change of HLA-E mRNA amount at any time point of culture from 30 min to 4 hr. RU486, an antagonist for progesterone receptor, added to the culture medium concomitantly with 1000 ng/mL of progesterone, diminished the effect of progesterone on HLA-E mRNA amount at 1 hr (Fig. 1b). These results indicated that progesterone increased HLA-E

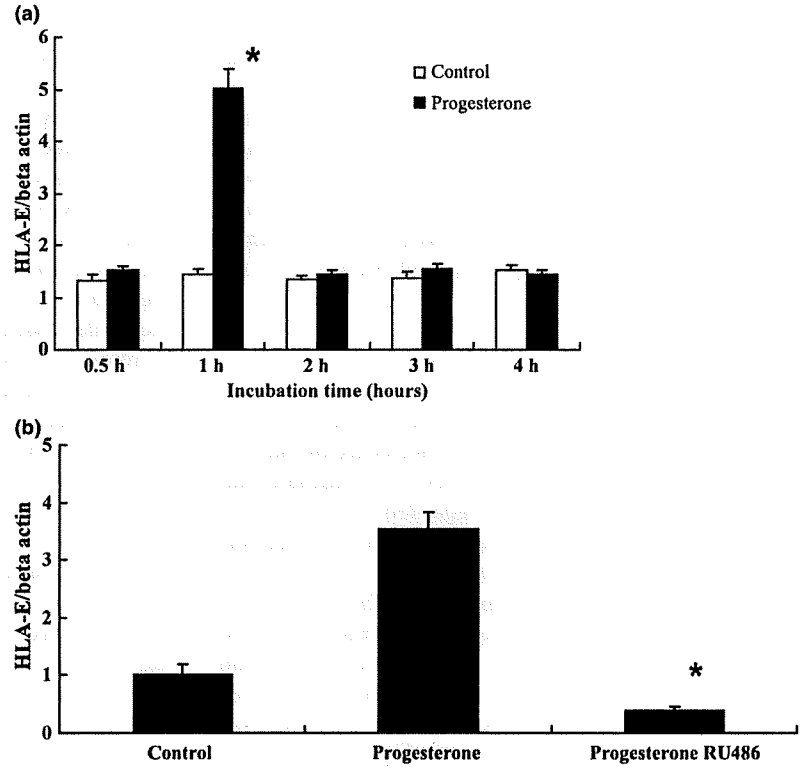

Fig. 1 The mRNA amount of HLA-E in JEG-3 cells was analyzed by real-time PCR. (a) The mRNA amount with or without progesterone was examined at different culture time (0.5, 1, 2, 3, 4 hours). In each histogram, values with progesterone are demonstrated as black columns and without progesterone as white columns. (b) The mRNA amount was examined at 1 hour culture with progesterone, both with progesterone and concomitant RU486, and without supplementation. Data are shown with standard error bar. Star mark shows there is significant difference.

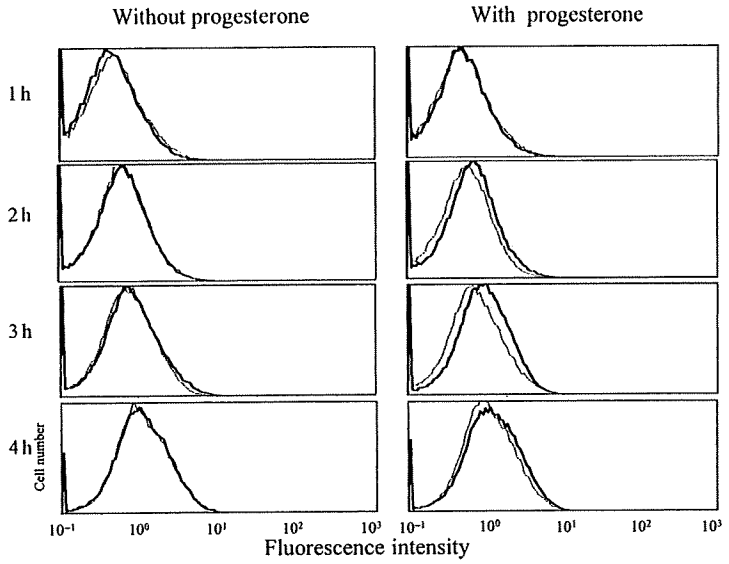

Fig. 2 Cell surface HLA-E protein expression on JEG-3 cells cultured with or without progesterone was analysed by flowcytometry using 3D12 at different culture time (1, 2, 3, 4 hours). In each histogram, values for 3D12 are demonstrated as a bold line and the negative control values as a dotted line.

mRNA expression in JEG-3 cells and RU486 diminished it.

Effect of Progesterone on Cell Surface HLA-E Protein Expression

Cell surface protein expression of HLA-E on JEG-3 cells treated with 1000 ng/mL of progesterone was investigated at several time points in culture by employing flow cytometric assay with anti-HLA-E monoclonal antibody, 3D12. The fluorescence intensity of progesterone-treated JEG-3 cells for 3D12 was slightly stronger than the control cells at 2, 3 and 4 hr (Fig. 2), indicating that progesterone slightly increased cell-surface expression of HLA-E on cultured JEG-3 cells.

Discussion

Human leukocyte antigen expression pattern of JEG-3 cells, a trophoblast-derived choriocarcinoma cell line, is so similar to that of EVTs in human placenta[15] that JEG-3 can be regarded as an *in vitro* model of EVTs to investigate the effect of progesterone on HLA expression on them.

The most outstanding finding in this study was that progesterone upregulated HLA-E mRNA expression in JEG-3 cells. This is the first demonstration that expression of HLA-E is controlled by steroid hormone. A significant mRNA increase was observed only at 1 hr in time course, indicating that the effect of progesterone was immediate and temporal. This finding is congruent with the previous report that direct activation of gene expression through steroid hormone receptor usually occurs within 1 through 4 hr.[16]

We further demonstrated that RU486 antagonized the reaction concerning HLA-E mRNA caused by progesterone, suggesting that the increase in HLA-E mRNA observed in progesterone treated cells was mediated by progesterone receptor (PR). In general, PR activated by progesterone starts to act as a transcription factor binding to progesterone response element (PRE) sequence in the promoter of target genes.[17] As no evidence showing that HLA-E gene promoter contains PRE sequence is currently available, further investigation is needed to elucidate the molecular pathway connecting PR activation and increase of HLA-E mRNA.

In this study, progesterone slightly induced the cell surface expression of HLA-E in JEG-3 cells, while no cell surface expression was detected without progesterone. One simple speculation is that the increase in HLA-E mRNA caused by progesterone contributed to intracellular amount of HLA-E protein, then directly leading to the increase in HLA-E cell surface expression. As previously reported, the surface expression of HLA-E in human trophoblasts may depend mainly on the expression of HLA-G and HLA-C, which provide nonamer peptides required for surface expression of HLA-E.[1,6,18] Considering this, the leader sequence peptide derived from

HLA-G gene product, which is reported to be enhanced by progesterone at mRNA and protein level,[13] might be another factor involved in the increased cell surface expression of HLA-E.

Human placenta daily secretes abundant progesterone up to a level of 300 mg.[19] Progesterone acts as an immunomodulator in pregnancy by blocking cytotoxic T-cell activity,[10] and suppressing NK cell activity.[9] However, according to the previous studies, PR mRNA is absent both in decidual NK cells,[20] and in peripheral blood mononuclear cells.[21] It is therefore unlikely that progesterone has direct influence on these cells. This study revealed that progesterone upregulated HLA-E gene expression, suggesting the reported progesterone effect on NK cell activity may partly be mediated by the modulation of HLA-E expression.

Uterine NK cells express high level of HLA-E specific receptor, CD94/NKG2 family molecules,[2] and besides, inhibitory CD94/NKG2A receptor binds to HLA-E with higher affinity than activating CD94/NKG2C receptor.[6,22] In the light of these facts, we can hypothesize that the increase in cell surface HLA-E expression on trophoblasts induced by progesterone may result in the suppression of the cytotoxic NK cell activity through the interaction with CD94/NKG2A receptor.

In summary, we demonstrated that progesterone upregulated HLA-E expression at mRNA level, and increased cell surface HLA-E expression in JEG-3. Although further investigation is required to see whether this reaction observed here also occurs in trophoblasts in placenta, our findings might give a new clue to the immunological mechanism supporting placental development.

References

1 King A, Burrows TD, Hiby SE, Bowen JM, Joseph S, Verma S, Lim PB, Gardner L, Le P, Ziegler A, Uchanska-Ziegler B, Loke YW: Surface expression of HLA-C antigen by human extravillous trophoblast. *Placenta* 2000; 21:376–387.

2 King A, Allan DS, Bowen M, Powis SJ, Joseph S, Verma S, Hiby SE, McMichael AJ, Loke YW, Braud VM: HLA-E is expressed on trophoblast and interacts with CD94/CDNKG2 receptors on decidual NK cells. *Eur J Immunol* 2000; 30:1623–1631.

3 Ishitani A, Sageshima N, Lee N, Dorofeeva N, Hatake K, Marquardt H, Geraghty DE: Protein expression and peptide binding suggest unique and interacting functional roles for HLA-E, F, and G in maternal-placental immune recognition. *J Immunol* 2003; 171:1376–1384.

4 Koller BH, Geraghty DE, Shimizu Y, DeMars R, Orr HT: HLA-E. A novel HLA class I gene expressed in resting T lymphocytes. *J Immunol* 1988; 141:897–904.

5 Lee N, Llano M, Carretero M, Ishitani A, Navarro F, Lopez-Botet M, Geraghty DE: HLA-E is a major ligand for the natural killer inhibitory receptor CD94/NKG2A. *Proc Natl Acad Sci USA* 1998; 95:5199–5204.

6 Llano M, Lee N, Navarro F, Garcia P, Albar JP, Geraghty DE, Lopez-Botet M: HLA-E-bound peptides influence recognition by inhibitory and triggering CD94/NKG2 receptors: preferential response to an HLA-G-derived nonamer. *Eur J Immunol* 1998; 28:2854–2863.

7 Borrego F, Ulbrecht M, Weiss EH, Coligan JE, Brooks AG: Recognition of human histocompatibility leukocyte antigen (HLA)-E complexed with HLA class I signal sequence-derived peptides by CD94/NKG2 confers protection from natural killer cell-mediated lysis. *J Exp Med* 1998; 187:813–818.

8 Navarro F, Llano M, Bellon T, Colonna M, Geraghty DE, Lopez-Botet M: The ILT2 (LIR1) and CD94/NKG2A NK cell receptors respectively recognize HLA-G1 and HLA-E molecules co-expressed on target cells. *Eur J Immunol* 1999; 29:277–283.

9 Hansen KA, Opsahl MS, Nieman LK, Baker JR Jr, Klein TA: Natural killer cell activity from pregnant subjects is modulated by RU 486. *Am J Obstet Gynecol* 1992; 166:87–90.

10 Mannel DN, Falk W, Yron I: Inhibition of murine cytotoxic T cell responses by progesterone. *Immunol Lett* 1990; 26:89–94.

11 Piccinni MP, Scaletti C, Maggi E, Romagnani S: Role of hormone-controlled Th1- and Th2-type cytokines in successful pregnancy. *J Neuroimmunol* 2000; 109:30–33.

12 Miyaura H, Iwata M: Direct and indirect inhibition of Th1 development by progesterone and glucocorticoids. *J Immunol* 2002; 168:1087–1094.

13 Yie SM, Li LH, Li GM, Xiao R, Librach CL: Progesterone enhances HLA-G gene expression in JEG-3 choriocarcinoma cells and human cytotrophoblasts in vitro. *Hum Reprod* 2006; 21:46–51.

14 Malmberg KJ, Levitsky V, Norell H, de Matos CT, Carlsten M, Schedvins K, Rabbani H, Moretta A, Söderström K, Levitskaya J, Kiessling R: IFN-gamma protects short-term ovarian carcinoma cell lines from CTL lysis via a CK94/NKG2A-dependent mechanism. *J Clin Invest* 2002; 110:1515–1523.

15 Gobin SJ, Wilson L, Keijsers V, Van den Elsen PJ: Antigen processing and presentation by human trophoblast-derived cell lines. *J Immunol* 1997; 158:3587–3592.
16 Landers JP, Spelsberg TC: New concepts in steroid hormone action: transcription factors, proto-oncogenes, and the cascade model for steroid regulation of gene expression. *Crit Rev Eukaryot Gene Expr* 1992; 2:19–63.
17 Shanker YG, Rao AJ: Progesterone receptor expression in the human placenta. *Mol Hum Reprod* 1999; 5:481–486.
18 Bhalla A, Stone PR, Liddell HS, Zanderigo A, Chamley LW: Comparison of the expression of human leukocyte antigen (HLA)-G and HLA-E in women with normal pregnancy and those with recurrent miscarriage. *Reproduction* 2006; 131:583–589.
19 Ben-Zimra M, Koler M, Melamed-Book N, Arensburg J, Payne AH, Orly J: Uterine and placental expression of steroidogenic genes during rodent pregnancy. *Mol Cell Endocrinol* 2002; 187:223–231.
20 Henderson TA, Saunders PT, Moffett-King A, Groome NP, Critchley HO: Steroid receptor expression in uterine natural killer cells. *J Clin Endocrinol Metab* 2003; 88:440–449.
21 Schust DJ, Anderson DJ, Hill JA: Progesterone-induced immunosuppression is not mediated through the progesterone receptor. *Hum Reprod* 1996; 11:980–985.
22 Kaiser BK, Barahmand-Pour F, Paulsene W, Medley S, Geraghty DE, Strong RK: Interactions between NKG2x immunoreceptors and HLA-E ligands display overlapping affinities and thermodynamics. *J Immunol* 2005; 174:2878–2884.

Cancer Science
The official journal of the Japanese Cancer Association JCA

Novel human papillomavirus type 18 replicon and its application in screening the antiviral effects of cytokines

Ayano Satsuka,[1,2] Satoshi Yoshida,[1,3] Naoko Kajitani,[1,2] Hiroyasu Nakamura[1,3] and Hiroyuki Sakai[1,4]

[1]Laboratory of Gene Analysis, Department of Viral Oncology, Institute for Virus Research; [2]Laboratory of Mammalian Molecular Biology, Graduate School of Bioscience; [3]Department of Viral Oncology, Graduate School of Medical Sciences, Kyoto University, Kyoto, Japan

(Received June 29, 2009/Revised October 9, 2009/Accepted October 19, 2008)

Human papillomaviruses (HPVs) infect the stratified epithelial organ. The infection induces benign tumors, which occasionally progress into malignant tumors. To elucidate the virus-induced tumorigenesis, an understanding of the lifecycle of HPV is crucial. In this report, we developed a new system for the analysis of the HPV lifecycle. The new system consists of a novel HPV replicon and an organotypic "raft" culture, by which the HPV-DNA is maintained stably in normal human keratinocytes for a long period and the viral vegetative replication is reproduced. This system will benefit biochemical and genetic studies on the lifecycle of HPV and tumorigenesis. This system is also valuable in screening for antiviral compounds. We confirmed its usefulness by evaluating the antivirus effect of cytokines. (*Cancer Sci* 2009)

The infection of high-risk type human papillomavirus (HPV) is a major risk factor for cervical cancer.[1–3] The World Health Organization has reported that the cases of HPV-associated cancers number about half a million, which corresponds to 10% of cancer cases in women.[4] This indicates the importance of the prevention of and urgently developing treatment for the cancer.

In order to control cervical cancer, it is essential to understand the regulatory mechanisms of the HPV infection. The primary target for HPV infection is the epithelial cells (keratinocytes) of the stratified squamous epithelium, and replication of HPV is strictly regulated by the differentiation program of the keratinocytes,[5] making it difficult to analyze the virus lifecycle in standard tissue culture systems. Several tissue culture conditions have been used for studying the differentiation-dependent lifecycle, such as a suspension culture of keratinocytes using methylcellulose "semisolid" medium,[6,7] a calcium-induced differentiation of keratinocytes,[8] and an organotypic raft culture.[9–11] Among them, the raft culture seems superior for studying the HPV lifecycle, because it is able to reproduce the stratified structure of epithelium, support the production of progeny virions in the differentiated layer, and capture the virus-induced hyperplasia as in the infected lesions. Although the raft culture has been successfully used for the analysis of the HPV lifecycle in combination with the genomic-type of HPV-DNA,[12] the drawbacks to using the culture system are the intricateness in the construction of it and the difficulty in obtaining the cell population maintaining the HPV-DNA.

In this manuscript, we tried to improve the suitability of the culture system for analysis of the HPV lifecycle. We constructed a new HPV replicon that could be maintained for a long period in comparison with the conventional method utilizing the genomic-type HPV-DNA. The raft culture system incorporating the new replicon could reproduce the physiological status of HPV-infected lesions: virus-induced hyperplasia accompanied by viral DNA amplification and late gene expression. This new system might accelerate the investigation of the HPV lifecycle. The usefulness of the system was verified by examining the effects of several cytokines on HPV replication and hyperplasia induction.

Materials and Methods

Construction of plasmid DNAs. HPV18 genomic DNA was isolated from a plasmid containing a full-length HPV18 DNA (GenBank accession no.: X05015). A new HPV18 replicon, p18FLneo, was constructed as illustrated in Figure 1. pEGFP1-ori(pBR) was constructed by replacing the origin of pEGFP1 (Clontech Laboratories, Mountain View, CA, USA) with pBR322-ori derived from pPUR (Clontech Laboratories). The long control region (LCR) of HPV18 (nucleotide number 7000 to 100; GenBank no.: X05015) was isolated by PCR, and then cloned into the vector pEGFP1-ori(pBR); the resultant plasmid was named 18LCR/pEGFP1-ori(pBR). Full-length HPV18 genome was cloned into the 18LCR/pEGFP1-ori(pBR) by using the *Afl*II recognition site. The genomic-type of HPV18 DNA was obtained by self-ligation of the full-length HPV18 DNA by following a method previously described.[13]

Cell culture and transfection. Human foreskin fibroblasts (HFFs) and human foreskin keratinocytes (HFKs) were commercially obtained (Kurabo Industries, Osaka, Japan), and maintained with 10% fetal bovine serum/DMEM and a serum-free keratinocyte growth medium (KGM) (EpiLife-KG2; Kurabo Industries), respectively. HFKs were transfected with 2 μg of p18FLneo or 1.5 μg of the genomic-type HPV18 DNA plus 0.5 μg of pEGFP1 by the nucleofection method (Nucleofector Kit; Amaxa, Cologne, Germany). The HFKs transfected with p18FLneo were cultured under the presence of G418 for more than 4 weeks, then used for the experiments.

Southern hybridization. Total DNA was extracted from the HFKs by following a standard protocol.[14] Five μg of the total DNA was digested with *Dpn*I and *Bgl*I, and then the DNA fragments were separated by 0.8% agarose gel electrophoresis, and transferred to a nylon membrane (Hybond N+; Amersham Biosciences UK, Little Chalfont, UK). For the detection of HPV18-specific DNA, a non-RI detection system was employed (Digoxigenin [DIG] Wash and Block Buffer Set and anti-DIG-alkaline phosphatase [AP]; Roche Diagnostics, Mannheim, Germany). The DIG-labeled probe for the LCR (7000–100 nt; GenBank no.: X05015) or L1 region (6137–7136 nt; GenBank no.: X05015) of HPV18 was obtained by a PCR-mediated method (PCR DIG Probe Synthesis Kit; Roche Applied Science, Manheim, Germany). The chemiluminescent signal

[4]To whom correspondence should be addressed.
E-mail: hsakai@virus.kyoto-u.ac.jp

doi: 10.1111/j.1349-7006.2009.01411.x

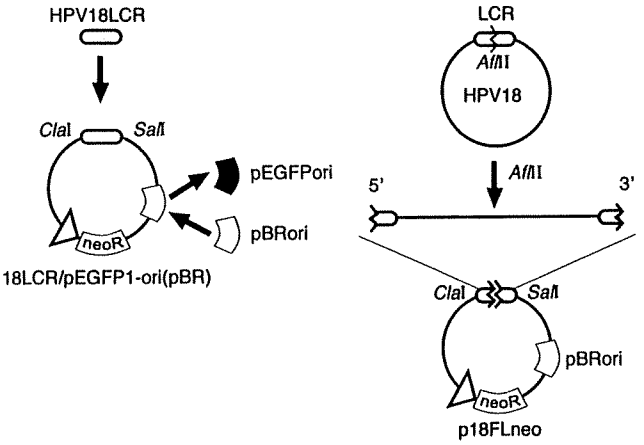

Fig. 1. Structure of a new human papillomavirus (HPV) replicon. A new replicon containing the full length of HPV18 genomic DNA constructed with a backbone plasmid, pEGFP1-ori(pBR), based on pEGFP1 plasmid. The replication origin (ori) element was replaced with that of pBR322. HPV18 long control region (LCR) was cloned into the pEGFP1-ori(pBR), and then the full-length HPV18 genome was inserted into the AflII site located in the LCR region. The obtained replicon was named p18FLneo.

was visualized with a chemiluminescent image analyzer (LAS-3000; Fuji Film, Tokyo, Japan).

Organotypic raft culture system. The construction of the organotypic raft culture and the preparation of frozen section have been described previously.[15–17] For BrdU incorporation, 50 g/mL BrdU (Sigma-Aldrich, St Louis, MO, USA) was added in the medium 6 h before harvest. The thickness of the epidermal layer was measured using image analysis software (AxioVision 3.1; Carl Zeiss Vision, Munich, Germany).

Immunoblot analysis. Total cell lysate of HFKs was obtained with a triple-detergent buffer (50 mM Tris-HCl [pH 8.0], 150 mM NaCl, 0.02% sodium azide, 0.1% sodium dodecyl sulfate [SDS], 1% Nonidet P-40, 0.5% sodium deoxycholate)[18] supplemented with a protease inhibitor cocktail (0.5 mM PMSF, 0.15 M aprotinin, 1 M E-64, 1 M leupeptin, 0.5 M EDTA) (Nakarai Tesuque, Kyoto, Japan) and 1 mM dithiothreitol. Equal amounts of cell lysate (5 μg protein) were subjected to SDS–polyacrylamide gel electrophoresis (SDS-PAGE) and the gel was blotted to a PVDF membrane (Hypond-P; Amersham Biosciences UK). The equalities of the loaded amounts were confirmed with the anti-actin immunoblot (1:50000) (clone AC-15; Sigma-Aldrich) (data not shown). Antibodies for p53 (1:1000) (Ab-6; Oncogene Research Products, San Diego, CA, USA) and pRb (1:1000; BD Biosciences Pharmingen, San Diego, CA, USA) were purchased commercially. Horseradish peroxidase (HRP)-conjugated secondary antibodies (1:3000; Amersham Biosciences UK) and a luminal reagent (Western Blotting Luminol Reagent; Santa Cruz Biotechnology, Santa Cruz, CA, USA) were purchased commercially. The chemiluminescent signal was visualized with a chemiluminescent image analyzer (LAS-3000; Fuji Film).

Immunohistochemistry (IHC). IHC for the tissue sections on slide glasses was performed as described previously.[15–17] Antibodies for BrdU (1:400) (clone 2B-1; MBL, Nagoya, Japan) and L1 (1:200) (MAB837; Millipore, Billerica, MA, USA), and p53 (Ab-6) (Oncogene Research Products), and pRb (BD Biosciences Pharmingen) were purchased commercially.

***In situ* hybridization (ISH).** Detection of HPV18 DNA signals in the tissue sections was performed with the TSA-biotin system (Perkin-Elmer, Boston, MA, USA) following the manufacturer's instructions. The DIG-labeled DNA for HPV18 LCR region (7000–100 nt; GenBank no.: X05015) (DIG high prime; Roche Diagnostics) was used as the probe. For the detection of DIG-labeled probe, HRP-labeled anti-DIG antibody (Dako, Glostrup, Denmark) was used. After hybridization, biotinyl tyramide working solution, SA-HRP (streptavidin–HRP), and metal-enhanced DAB solution (Roche Diagnostics) was used for detection of the signal. All slides were counterstained with hematoxylin.

Cytokine treatment. In monolayer culture, HFKs were incubated with cytokines (interferon [IFN]-β, 100 units/mL; transforming growth factor [TGF]-β, 1 ng/mL; tumor necrosis factor [TNF]-α, 5 ng/mL) for 3 days. IFNβ and TGFβ (Sigma-Aldrich) and TNFα (Merk Biosciences, San Diego, CA, USA) were purchased from the distributors. In the organotypic raft culture, cytokines were added in the culture medium for 7 days before the sample harvest.

Apoptosis induction by cytokine. 2×10^5 cells were cultured in the growth medium supplemented with the cytokines for 3 days. The treated cells were washed, trypsinized, and fixed with ice-cold methanol. Apoptotic cells were labeled by M30 antibody (CytoDEATH; Roche Diagnostics) and AlexaFLUOR488-antimouse antibody (Invitrogen, Carlsbad, CA, USA), and then counted by flow cytometry (BD Biosciences, San Jose, CA, USA).

Results

Construction of new HPV replicon. Genomic-type HPV-DNA was used as the replicon to obtain the keratinocytes maintaining HPV-DNA. The genomic-type DNA, which was constructed by re-circularization of full-length HPV-DNA, was transfected into the cells with the pSV2*neo* expressing a neomycin-resistance gene (neo^R).[13] The transfected cells were selected in the culture medium containing G418 for about 1 week, and then the surviving cells were expanded without the drug selection. The raft culture constructed with the cells could reproduce viral vegetative replication as reported previously.[12] By this method, there is no selectable pressure for the maintenance of HPV-DNA, causing a possible problem in that the cells lose HPV-DNA. It was also suggested that the transfection of the genomic-type DNA was inefficient because of its non-supercoiled structure.[19] To eliminate this potential problem, full-length HPV18 DNA was inserted into a plasmid containing the neo^R expression unit (Fig. 1). The replication of HPVs is regulated by the LCR as the promoter/enhancer for gene expressions at the 5′ region of the coding region and as the transcriptional terminator at the 3′ region. Therefore, the LCR was added at the both sides of the coding region. We named the new replicon p18FLneo (FL is an abbreviation for full length).

We verified the potential of p18FLneo as the replicon by examining whether it could be maintained stably in culture cells. HFKs were transfected with p18FLneo, then cultured under the presence of G418 for 4 weeks. Under the same condition, we found that the mock-transfected cells were dislodged within a week and that the cells transfected with pEGFP1, which contains the neo^R expression unit and is replication-defective in the HFKs, could not survive for more than 2 weeks. The total DNAs were collected from the cells, and then HPV-DNA was detected by Southern hybridization analysis. The result indicated that p18FLneo was stably maintained in the HFKs as a HPV18 replicon (Fig. 2A, p18FLneo). In order to validate its potential as the replicon, the genomic-type of HPV18 DNA was used as the control replicon (Fig. 2A, 18-ligation). The genomic-type HPV18 was introduced with the pEGFP1 into the HFKs. The transfected cells were selected under the presence of G418 for 1 week, and then the surviving cells were cultured without the drug-selection for 3 weeks. The amount of replicated HPV-DNA was analyzed by Southern blot analysis, and it appeared that the efficiency of the maintenance or the replication of the genomic-type HPV18

doi: 10.1111/j.1349-7006.2009.01411.x

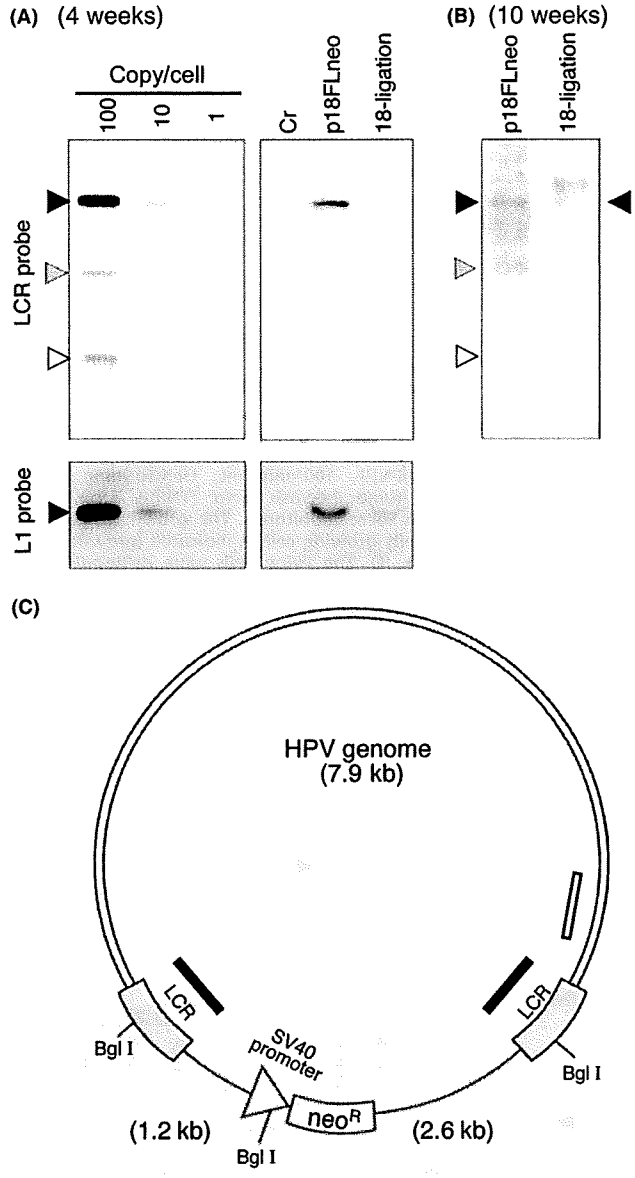

Fig. 2. Maintenance of the new human papillomavirus (HPV) replicon in primary keratinocytes. (A) Maintenance of the HPV replicon in the human foreskin keratinocytes (HFKs) 4 weeks after transfection was examined by Southern blot analysis. Total DNA was extracted from the normal HFKs (Cr), the HFKs harboring either the HPV replicon (p18FLneo) or the genomic-type HPV18 DNA (18-ligation) and subjected to *DpnI* + *BglI* digestion. Each lane was loaded with 5 μg of the total DNA. p18FLneo DNA was used as the control for the copy number per cell. p18FLneo was digested with *BglI* and applied to the agarose gel at an amount equivalent to 1 copy, 10 copies, or 100 copies per cell. The probe used for the detection of HPV-DNA was DIG-labeled 18LCR or 18L1 DNA fragment. Closed triangle indicates the position of the full-length HPV18 genomic DNA. Gray and open triangles indicate the positions of the fragments containing a portion of long control region (LCR) and the backbone plasmid; those fragments could not be detected with L1 probe. (B) The maintenance of the HPV replicon in HFKs 10 weeks after transfection was examined as described in (A). Closed triangle indicates the position of the full-length HPV18 genomic DNA. Gray and open triangles indicate the positions of the fragments containing a portion of LCR and the backbone plasmid. The extra signals observed in each lane were considered the integrated form of HPV-DNA. (C) The scheme of pFL18neo. Gray region indicates HPV18 DNA. Black and white bars indicate the regions targeted by LCR and L1 probes, respectively. The recognition sites for BglI are indicated, and the digestion produced three DNA fragments, 7.9 kb, 2.6 kb, and 1.2 kb.

DNA was lower than that of p18FLneo. These results suggested the advantage of p18FLneo as the HPV replicon.

The HFKs containing p18FLneo could be maintained for more than 10 weeks under the presence of G418. The growth potential of normal HFKs apparently declined after 6 weeks of culturing and the cells acquired senescence status, indicating that the HFKs containing p18FLneo were immortalized by the functions of HPV E6 and E7. The existence of HPV-DNA in the cells was examined, and it was revealed that the majority of HPV-DNA was maintained as the episomal status and that some portion of the DNA might be integrated in the host chromosome (Fig. 2B, p18FLneo). In the accompanying experiment, the DNA status in the HFKs containing the genomic-type HPV-DNA was examined, and it found that most of the HPV-DNA was maintained as integrated form (Fig. 2B, 18-ligation).

Raft culture with HFKs harboring the new HPV replicon. The HFKs or the spontaneously immortalized keratinocytes (normal immortal keratinocytes, NIKS)[20] harboring HPV genomic DNA were used to organize the organotypic raft culture,[11,13,21,22] and they could support HPV replication in a differentiation-dependent manner. We examined whether the HFKs maintaining p18FLneo ($HFK_{p18FLneo}$) could also support the HPV lifecycle in the raft culture.

$HFK_{p18FLneo}$ could organize a stratified epithelial structure and it appeared that significant hyperplasia was induced (Fig. 3, H&E). In the epithelial layer of the $HFK_{p18FLneo}$ raft culture, BrdU-positive cells were detected in the parabasal layer. On the contrary, BrdU-positive cells were restricted at the basal layer in the raft culture with normal HFKs (Fig. 3, BrdU). This observation suggested that p18FLneo had the potential to disturbe the differentiation program of the epithelial cells and induced hyperproliferation.

We next examined whether the late-phase of the virus lifecycle was reproduced with $HFK_{p18FLneo}$. By ISH with the HPV18 probe, the cells positive for HPV18 DNA were detected in the suprasurface layer (Fig. 3, ISH), indicating that the copy number of p18FLneo was amplified in the differentiated layer of the epithelium. The expression of the late gene product, L1, was also detected in the differentiated layers by IHC (Fig. 3, IHC). These observations indicate that $HFK_{p18FLneo}$ in combination with the raft culture is an appropriate tool for the analysis of the HPV lifecycle. Although the $HFK_{p18FLneo}$ maintained for long period (10 weeks) was also used for the raft culture, it failed to organize a stratified epithelial layer, indicating it lost the property of normal cellular differentiation.

Application of the new HPV replicon: (1) Effects of cytokines on the latent phase of HPV infection. Cytokine production is a biological response *in vivo* to virus infection or inflammation. One of the cytokines, type I IFN, is used in chemotherapy for HPV-positive cervical neoplasia.[23] Other cytokines, TGFβ and TNFα, have been reported to be involved in the response to HPV infection.[24–30] We examined the effects of these cytokines on HPV replication using the new HPV replicon system.

The monolayer culture of $HFK_{p18FLneo}$ is supposed to represent the status of the latent infection of HPV in basal cells. We first examined the effects of the cytokines on the $HFK_{p18FLneo}$ monolayer culture. We chose doses of cytokines that had minimal effects on the growth of normal HFKs (IFNβ, 100 units/mL; TGFβ, 1 ng/mL; TNFα, 5 ng/mL) in order to observe the specific effects on HPV replication (Fig. 4). These doses of the cytokine treatments had also no significant effects on the growth of $HFK_{p18FLneo}$. The apoptosis induction by the cytokines was also examined by FACS analysis using an apoptosis-specific antibody (M30 CytoDEATH; Roche Diagnostics), and it appeared that these cytokine treatments did not induce any apoptotic response (data not shown). Note that the treatment of higher doses of the cytokines induced growth arrest or

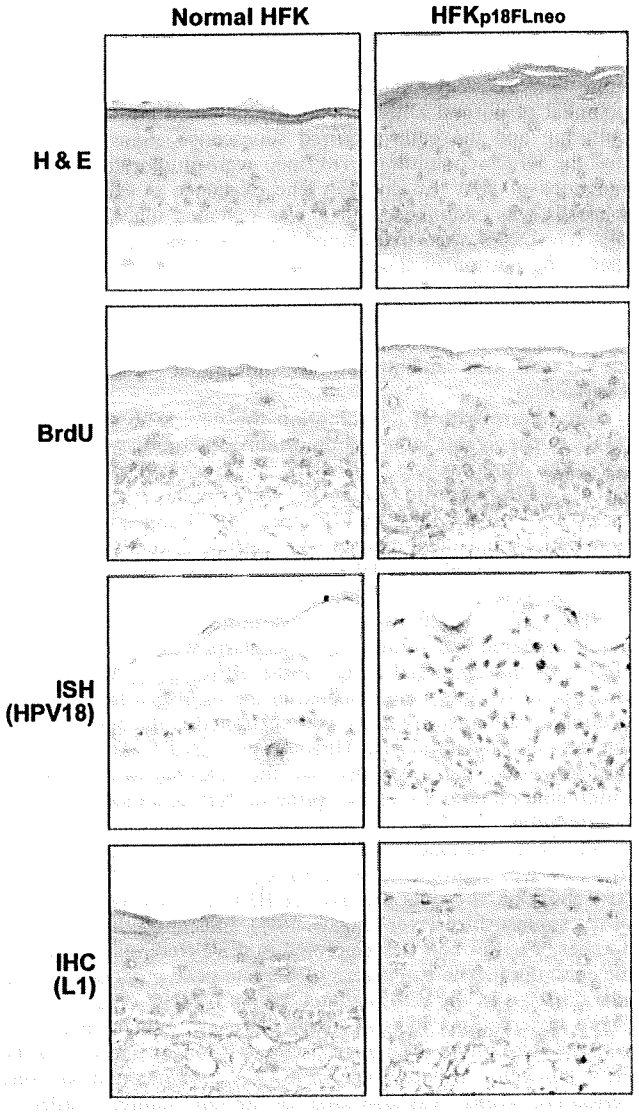

Fig. 3. Vegetative replication of the human papillomavirus (HPV) replicon in the raft culture. Thin sections (7 μm) were obtained from the raft culture organized with normal human foreskin keratinocytes (HFKs) and $HFK_{p18FLneo}$. The DNA synthesis of the cell was monitored by immunohistochemistry for incorporated BrdU. HPV18 DNA was detected by *in situ* hybridization (ISH) with DIG-labeled L1 probe. The expression of L1 protein was analyzed by IHC with anti-L1 antibody.

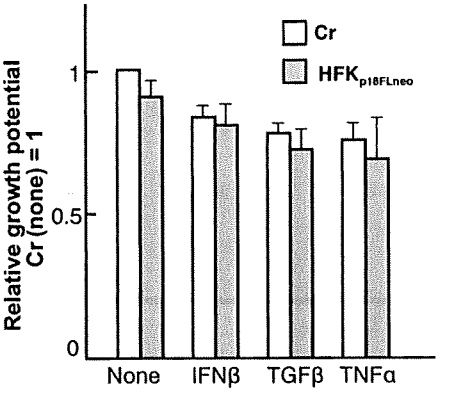

Fig. 4. Effects of cytokines on the proliferation of human foreskin keratinocytes (HFKs) harboring p18FLneo. The effects of cytokine treatments (interferon [IFN]-β, 100 units/mL; transforming growth factor [TGF]-β, 1 ng/mL; tumor necrosis factor [TNF]-α, 5 ng/mL) on the proliferation of HFKs were monitored. The growth rate in 72-h culture of the exponentially growing cells is indicated (growth rate of not treated normal HFKs, 1). The living cells were distinguished by Trypan blue exclusion. The value is the average of at least three independent experiments and the SD is indicated.

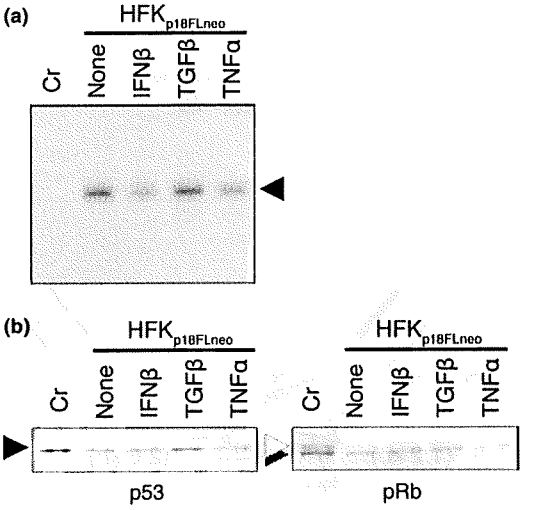

Fig. 5. Effects of cytokines on the maintenance of the human papillomavirus (HPV) replicon. (A) The $HFK_{p18FLneo}$ was treated with cytokines for 3 days and total DNA was extracted. The DNA was digested with both BglI and DpnI and 2 μg of it was subjected to Southern blot analysis with the DIG-labeled L1 probe. Normal human foreskin keratinocytes (HFKs) were used as the control (Cr). (B) Expressions of p53 and pRb in the same cells monitored by immunoblot analysis.

apoptotic cell death of both normal HFKs and $HFK_{p18FLneo}$ (data not shown).

Next, we examined the effects of the cytokines on the maintenance of HPV-DNA in $HFK_{p18FLneo}$, and the result indicated that IFNβ treatment moderately suppressed HPV-DNA replication (Fig. 5A). The TGFβ and TNFα treatments did not influence DNA maintenance significantly. In HPV-infected cells, the expressions of cellular tumor suppressors p53 and pRb are suppressed by the functions of viral oncoproteins E6 and E7, respectively. We analyzed the expressions of p53 and pRb in $HFK_{p18FLneo}$ by immunoblot analysis, and found that they slightly decreased as compared with those in the normal HFKs (Fig. 5B). This weak suppression indicated that the expression levels of the viral oncoproteins were kept low as found in the latent infection of HPV. The weak suppressions of p53 and pRb expressions were not modified significantly by the cytokine treatments.

The results indicated that the cytokine treatments used in this report did not affect the growth potential of $HFK_{p18FLneo}$ and the maintenance of HPV-DNA. Given that $HFK_{p18FLneo}$ is considered to represent basal cells latently infected with HPV, these results suggested that the cytokine treatments had no anti-HPV effect on the latently infected cells.

Application of the new HPV replicon: (2) Effects of cytokines on the late-stage of the HPV lifecycle. We next examined the effect of the same set of cytokines on the late-stage of the HPV lifecycle by using $HFK_{p18FLneo}$ and the raft culture. As described above, the raft culture with $HFK_{p18FLneo}$ showed a moderate hyperplasia at the epithelial layer (Fig. 3), and the hyperplasia

doi: 10.1111/j.1349-7006.2009.01411.x

could be suppressed by the IFNβ treatment to the level of normal HFKs (Fig. 6). The number of BrdU-positive cells in the upper layers of epithelium was decreased with IFNβ treatment (Fig. 7, BrdU). As compared with IFNβ, the moderate but significant suppression could be also observed with TGFβ. In contrast, the TNFα could not suppress hyperplasia formation and it activated the invasive potential of the epithelial cells. The number of BrdU-positive cells was rather increased with TNFα. These results indicated that IFNβ treatment had an apparent suppressive effect on virus-induced hyperplasia. The results also raised the possibility that TNFα treatment accelerated virus-induced tumorigenesis.

Next, the effect of the cytokine treatment on the vegetative viral replication was analyzed. The amplification of viral DNA at the upper layer of epithelium was suppressed by the treatment of IFNβ and TGFβ (Fig. 7, ISH). On the other hand, TNFα treatment activated viral DNA amplification in the broad area of the epithelium. These observations indicated that both IFNβ and TGFβ could suppress the late phase in the HPV lifecycle and TNFα treatment had the opposite effect on it.

It is considered that the viral oncoproteins E6 and E7 are responsible for virus-induced hyperplasia.[31] We examined the effects of cytokines on the status of p53 and pRb in the raft culture in order to estimate the expression levels of E6 and E7, respectively. The expressions of p53 and pRb were decreased in the epithelial layer of the $HFK_{p18FLneo}$ raft culture as compared to those of normal HFKs (Fig. 7, p53 and pRb). It was supposed that this decrement was caused by the E6 and E7 expressed moderately in $HFK_{p18FLneo}$. IFNβ treatment recovered p53 expression at the middle layers of epithelium, although TGFβ did not modify the p53 status. TNFα enhanced p53 expression in the epithelium broadly. pRb expression was slightly recovered by all three cytokine treatments. These results indicated that the cytokines affected the expressions of p53 and pRb, although their relation to the antiviral effect remains unclear.

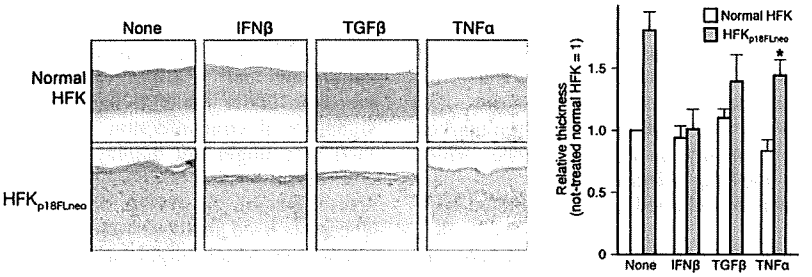

Fig. 6. Effects of cytokines on the raft culture constructed with human foreskin keratinocyte $(HFK)_{p18FLneo}$. Effects of cytokine treatments on the raft culture organized with normal HFKs or $HFK_{p18FLneo}$ were examined. Frozen-sections of the raft culture were fixed with 4% paraformaldehyde and stained with H&E. The thickness of the epidermis was estimated by microscopic analysis with an image analysis application (AxioVision; Carl Zeiss Vision), and the relative values are indicated as a bar chart (thickness of not treated normal HFK set as 1.0; average value, 95 μm). The value is the average of at least three independent experiments and the SD is indicated. Note that the epidermis of the $HFK_{p18FLneo}$ treated with tumor necrosis factor (TNF)-α exhibited the invasion phenotype; therefore, the thickness of it could not be measured precisely (indicated with an asterisk).

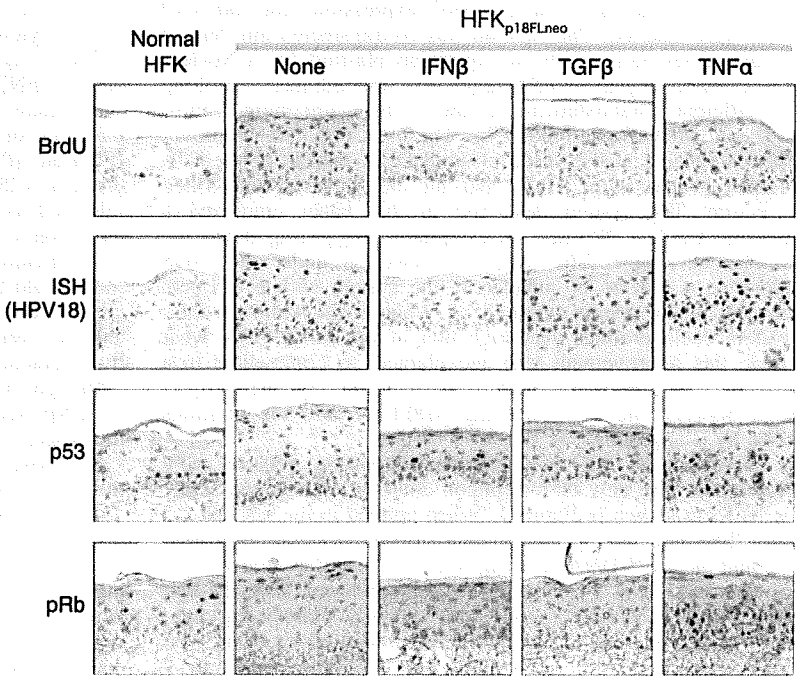

Fig. 7. The effects of cytokine treatments on human papillomavirus (HPV) replication. Effects of cytokine treatments on HPV replication and on cellular status were examined by using the raft culture. The DNA synthesis of the cells was monitored by the uptake of BrdU. Incorporated BrdU was detected by immunohistochemistry (IHC) with anti-BrdU antibody. HPV-DNA was detected by *in situ* hybridization (ISH) with DIG-labeled 18L1 probe (ISH). The expressions of p53 and pRb in the raft culture were monitored by IHC with specific antibodies (p53 & pRb).

Discussion

A novel HPV replicon. We constructed a new replicon of HPV by integrating several improvements for the stable maintenance of the replicon in the cells, which made it easy to collect cells harboring HPV-DNA. The major points are summarized below.

- The HPV replicon has a configuration of plasmid DNA, not of genomic DNA. In previous reports, the genomic-type of DNA was used as a replicon. To obtain the genomic-structure of DNA, full-length HPV-DNA was excised from a plasmid and circularized by self-ligation.[13] This process is laborious and it is difficult to control the quality of the DNA, which influences the transfection efficiency. The self-ligated DNA has a non-supercoiled configuration, and such a form of DNA might not be an appropriate substrate for gene expression and DNA replication. We incorporated, therefore, the HPV-DNA into a plasmid backbone, which made it easier to control the DNA quality and the constancy of the transfection efficiency was improved.
- In the conventional protocol for obtaining the HFKs harboring HPV-DNA, HFKs were transfected with both the genomic-type of DNA and a plasmid expressing a drug-resistance gene, such as pSV2*neo*.[13] After a short period of drug selection, the cells were then expanded without drug selection. The HPV replicon used in this report contained a selection marker, an expression unit for a neomycin-resistance gene, which made it possible to apply the drug-selection even in the expansion process, ensuring that the obtained cells maintained HPV replicons.

In addition to these points, it is unique that p18FLneo contains the LCR at both sides of the genome (Fig. 1). Although we designed it by taking into account the roles of the LCR as 5′- and 3′-regulatory elements, the artificial structure might have unexpected effects on HPV replication. It is necessary, therefore, to compare carefully the replication potentials between the genomic-type DNA and p18FLneo. We also need to determine whether the 3′-LCR unit is required for the maintenance or vegetative replication of HPV-DNA.

Recently Wang *et al.* reported a new system for analyzing the HPV18 lifecycle.[19] They used a plasmid containing HPV18 genome into which a neo^R expression unit and loxP sites were inserted. The plasmid was co-transfected into human keratinocytes along with an expression plasmid for a Nuclear Localization Signal (NLS)-tagged Cre recombinase, resulting in efficient establishment of the cells maintaining almost authentic HPV18 genomic DNA. The most important improvement seemed that they used plasmid DNA instead of the self-ligated genomic-type DNA that did not have a supercoiled structure. The system described in this paper employed a plasmid DNA, p18FLneo, as a replicon, suggesting it has the similar advantage. The long-term selection under the G418 presence is able to be adapted in the system with p18FLneo, but not in the system reported by Wang *et al.* Although their system could produce very high titer of infectious virus, what made this improvement was unexplained, as commented in a review.[32] It will be necessary to perform side-by-side comparison between the systems using p18FLneo and the plasmids used by Wang *et al.*

Usefulness of the new system supporting efficient HPV replication. The new HPV replicon could be maintained stably in HFKs as shown in Figure 2. When applied in the raft culture, the HFKs maintaining the replicon showed moderate hyperplasia and the HPV-DNA was amplified at the differentiated layer of epidermis (Fig. 3). The hyperplasia observed with the raft culture was moderate as compared with that induced by high-risk type E7 expression.[16] The immunoblot analysis of p53 and pRb expressions in the HFKs indicated that the introduction of the HPV replicon suppressed moderately those expressions, suggesting the E6 and E7 expression levels in the HFKs were maintained at low level. It is supposed that the expressions of E6 and E7 are up-regulated in the course of malignant conversion of the HPV-infected cells,[33] thus, the raft culture harboring the HPV replicon seems to represent an early stage of the tumor induced by the HPV infection.

Effects of cytokines in protection against virus infection. Living organisms have protection systems for the viral infections. In mammals, a variety of cytokines are produced by either infected cells or periphery cells, which act in the elimination of the infected cells.[34] The system using the new HPV replicon and the raft culture could be used to examine the effect of cytokine treatment on the early stage of HPV-infected lesions. We selected three cytokines, IFNβ, TNFα, and TGFβ, because there were several reports indicating the relation between these cytokines and HPV infection.[24–30,35,36]

We first examined the effects of the cytokines on the monolayer culture of the HFKs harboring the HPV replicon, which represented the status of the HPV-infected basal cells. Under this condition, although IFNβ treatment could suppress HPV-DNA replication moderately, the treatments of other cytokines, TGFβ and TNFα, had almost no effect on both HPV-DNA replication and cell proliferation (Figs 4,5). HFKs harboring the 18FLneo under the monolayer culture condition showed little signature of viral infection, and the cytokine treatments examined here might not display their effect on such cells. On the contrary, it has been reported that these cytokines have suppressive effects on the growth of HPV-positive cell lines.[24–27,35,36] The cells used in those reports have malignant or transformed phenotype, which might have cause observations different from ours.

Next, the effects were examined using the raft culture (Fig. 6). Under this condition, IFNβ exhibited strong inhibitory effects on dysplasia formation. It also suppressed the vegetative replication of the virus in the suprabasal layer of epithelium. TGFβ also exhibited a significant inhibitory effect on both dysplasia formation and HPV-DNA amplification, but the effect was not as drastic as that of IFNβ. In contrast, it appeared that TNFα treatment enhanced HPV replication and induced the invasion of epithelial cells into the dermal layer.

IFNβ has been administered to HPV-infected lesions including condylomas and early stage cervical intraepithelial neoplasia [23] By using this model, it was possible to confirm the effectiveness of IFNβ on the treatment of HPV-related lesions under tissue culture condition, indicating that this system is a useful platform for examination of the detailed action-mechanisms of IFNβ on HPV replication. Recently, it was reported that p56, a product of ISG56, interacted with viral replication factor E1 and inhibited its function.[37] It will be interesting to examine the induction level of p56 by IFNβ treatment in both the monolayer and raft cultures.

It should be noted that the expressions of E6 and E7 are usually up-regulated in the advanced stages of cervical neoplasia, and they were reported to interfere with the IFN-related pathway by interacting with Tyk2,[38] IRF3,[39] IRF1,[40] or IRF9.[41] Although this report described the significant anti-HPV effects of IFNβ, such effects might be diminished in association with the progression of malignant status.

The observation that TNFα treatment enhanced HPV replication suggests that the inflammatory response accompanied by TNFα production exerts effects opposite to the antiviral response at the early stage of HPV-infected lesions. In searching for new therapeutic approaches to HPV-related diseases, it might be important to consider the induction of inflammation, which has the potential to accelerate disease progression.

In this report, we developed a new experimental system that could support the replication of HPV-DNA for a long period

doi: 10.1111/j.1349-7006.2009.01411.x

and the differentiation-dependent lifecycle of the virus. This system will be adapted to screening for other anti-HPV compounds. It also allows the manipulation of the genetic elements of both host cells and virus; thus, the analysis of regulatory mechanisms of the virus lifecycle and virus-induced tumorigenesis becomes accessible.

Acknowledgments

We thank the many colleagues for technical assistance and manuscript preparation, K. Sasaki for essential advice and support, Dr. P.M. Howley for providing full-length clones for HPV18, and Dr. M. Tsunenaga and Dr. T. Kuroki for instructions regarding the organotypic raft culture. This work is supported in part by a Grant-in-Aid from the Ministry of Health, Labor and Welfare of Japan for the Third-Term Comprehensive 10-year Strategy for Cancer Control. A.S., S.Y., N.K., and H.N. were supported by the 21st Century COE program of the Japan Society for the Promotion of Science (JSPS).

References

1 Howley PM, Lowy DR. Papillomavirus and their replication. In: Knipe DM, Howley PM, eds. *Fields Virology*, 5th edn. Hagerstown: Lippincott Williams & Wilkins,a Wolters Kluwer Business, 2007; 2299–354.
2 Durst M, Gissmann L, Ikenberg H, Zur Hausen H. A papillomavirus DNA from a cervical carcinoma and its prevalence in cancer biopsy samples from different geographic regions. *Proc Natl Acad Sci U S A* 1983; **80**: 3812–5.
3 Zur Hausen H. Papillomavirus infections–a major cause of human cancers. *Biochim Biophys Acta* 1996; **1288**: F55–78.
4 Castellsagué X, De Sanjosé S, Aguado T *et al.* HPV and cervical cancer in the 2007 report. *Vaccine* 2007; **25** (Suppl 3): C1–230.
5 Longworth MS, Laimins LA. Pathogenesis of human papillomaviruses in differentiating epithelia. *Microbiol Mol Biol Rev* 2004; **68**: 362–72.
6 Flores ER, Lambert PF. Evidence for a switch in the mode of human papillomavirus type 16 DNA replication during the viral life cycle. *J Virol* 1997; **71**: 7167–79.
7 Adams JC, Watt FM. Fibronectin inhibits the terminal differentiation of human keratinocytes. *Nature* 1989; **340**: 307–9.
8 Ruesch MN, Laimins LA. Human papillomavirus oncoproteins alter differentiation-dependent cell cycle exit on suspension in semisolid medium. *Virol* 1998; **250**: 19–29.
9 Meyers C, Frattini MG, Hudson JB, Laimins LA. Biosynthesis of human papillomavirus from a continuous cell line upon epithelial differentiation. *Science* 1992; **257**: 971–3.
10 Dollard SC, Wilson JL, Demeter LM *et al.* Production of human papillomavirus and modulation of the infectious program in epithelial raft cultures. *OFF Genes Dev* 1992; **6**: 1131–42.
11 Frattini MG, Lim HB, Laimins LA. In vitro synthesis of oncogenic human papillomaviruses requires episomal genomes for differentiation-dependent late expression. *Proc Natl Acad Sci U S A* 1996; **93**: 3062–7.
12 Moody CA, Fradet-Turcotte A, Archambault J, Laimins LA. Human papillomaviruses activate caspases upon epithelial differentiation to induce viral genome amplification. *Proc Natl Acad Sci U S A* 2007; **104**: 19541–6.
13 Frattini MG, Lim HB, Doorbar J, Laimins LA. Induction of human papillomavirus type 18 late gene expression and genomic amplification in organotypic cultures from transfected DNA templates. *J Virol* 1997; **71**: 7068–72.
14 Strauss WM. Preparation of genomic DNA from mammalian tissue. In: Ausubel FM, Brent R, Kingston RE *et al.*, eds. *Current Protocols in Molecular Biology*. New York: John Wiley & Sons, Inc., 1998; 2.1–2.3.
15 Yoshida S, Kajitani N, Satsuka A, Nakamura H, Sakai H. Ras modifies proliferation and invasiveness of cells expressing human papillomavirus oncoproteins. *J Virol* 2008; **82**: 8820–7.
16 Ueno T, Sasaki K, Yoshida S *et al.* Molecular mechanisms of hyperplasia induction by human papillomavirus E7. *Oncogene* 2006; **25**: 4155–64.
17 Tsunenaga M, Kohno Y, Horii I *et al.* Growth and differentiation properties of normal and transformed human keratinocytes in organotypic culture. *Jpn J Cancer Res* 1994; **85**: 238–44.
18 Sambrool J, Fritsch EF, Maniatis T. *Molecular Cloning*. New York: Cold Spring Harbor Laboratory Press, 1989; 18.30–3.
19 Wang HK, Duffy AA, Broker TR, Chow LT. Robust production and passaging of infectious HPV in squamous epithelium of primary human keratinocytes. *Genes Dev* 2009; **23**: 181–94.
20 Allen-Hoffmann BL, Schlosser SJ, Ivarie CA, Sattler CA, Meisner LF, O'Connor SL. Normal growth and differentiation in a spontaneously immortalized near-diploid human keratinocyte cell line, NIKS. *J Invest Dermatol* 2000; **114**: 444–55.
21 Flores ER, Allen-Hoffmann BL, Lee D, Sattler CA, Lambert PF. Establishment of the human papillomavirus type 16 (HPV-16) life cycle in an immortalized human foreskin keratinocyte cell line. *Virol* 1999; **262**: 344–54.
22 Flores ER, Allen-Hoffmann BL, Lee D, Lambert PF. The human papillomavirus type 16 E7 oncogene is required for the productive stage of the viral life cycle. *J Virol* 2000; **74**: 6622–31.
23 Frazer IH, McMillan NAJ. Papillomatosis and condylomata acuminata. In: Penny S-HaRW, ed. *Clinical Applications of the Interferons*. London: Chapman and Hall Medical, 1997; 79–91.
24 Donalisio M, Cornaglia M, Landolfo S, Lembo D. TGF-beta1 and IL-4 downregulate human papillomavirus-16 oncogene expression but have differential effects on the malignant phenotype of cervical carcinoma cells. *Virus Res* 2008; **132**: 253–6.
25 Nindl I, Steenbergen RD, Schurek JO, Meijer CJ, Van der Valk P, Snijders PJ. Assessment of TGF-beta1-mediated growth inhibition of HPV-16- and HPV-18-transfected foreskin keratinocytes during and following immortalization. *Arch Dermatol Res* 2003; **295**: 297–304.
26 Villa LL, Vieira KB, Pei XF, Schlegel R. Differential effect of tumor necrosis factor on proliferation of primary human keratinocytes and cell lines containing human papillomavirus types 16 and 18. *Mol Carcinog* 1992; **6**: 5–9.
27 Vieira KB, Goldstein DJ, Villa LL. Tumor necrosis factor alpha interferes with the cell cycle of normal and papillomavirus-immortalized human keratinocytes. *Cancer Res* 1996; **56**: 2452–7.
28 Woodworth CD, McMullin E, Iglesias M, Plowman GD. Interleukin 1 alpha and tumor necrosis factor alpha stimulate autocrine amphiregulin expression and proliferation of human papillomavirus-immortalized and carcinoma-derived cervical epithelial cells. *Proc Natl Acad Sci U S A* 1995; **92**: 2840–4.
29 Kyo S, Inoue M, Hayasaka N *et al.* Regulation of early gene expression of human papillomavirus type 16 by inflammatory cytokines. *Virol* 1994; **200**: 130–9.
30 Zur Hausen H. Immortalization of human cells and their malignant conversion by high risk human papillomavirus genotypes. *Semin Cancer Biol* 1999; **9**: 405–11.
31 Dong W, Kloz U, Accardi R *et al.* Skin hyperproliferation and susceptibility to chemical carcinogenesis in transgenic mice expressing E6 and E7 of human papillomavirus type 38. *J Virol* 2005; **79**: 14899–908.
32 Galloway DA. Human papillomaviruses: a growing field. *Genes Dev* 2009; **23**: 138–42.
33 Munger K, Howley PM. Human papillomavirus immortalization and transformation functions. *Virus Res* 2002; **89**: 213–28.
34 Takeuchi O, Akira S. Recognition of viruses by innate immunity. *Immunol Rev* 2007; **220**: 214–24.
35 Stanley MA, Pett MR, Coleman N. HPV: from infection to cancer. *Biochem Soc Trans* 2007; **35**: 1456–60.
36 Koromilas AE, Li S, Matlashewski G. Control of interferon signaling in human papillomavirus infection. *Cytokine Growth Factor Rev* 2001; **12**: 157–70.
37 Terenzi F, Saikia P, Sen GC. Interferon-inducible protein, P56, inhibits HPV DNA replication by binding to the viral protein E1. *EMBO J* 2008; **27**: 3311–21.
38 Li S, Labrecque S, Gauzzi MC *et al.* The human papilloma virus (HPV)-18 E6 oncoprotein physically associates with Tyk2 and impairs Jak-STAT activation by interferon-alpha. *Oncogene* 1999; **18**: 5727–37.
39 Ronco LV, Karpova AY, Vidal M, Howley PM. Human papillomavirus 16 E6 oncoprotein binds to interferon regulatory factor-3 and inhibits its transcriptional activity. *Genes Dev* 1998; **12**: 2061–72.
40 Perea SE, Massimi P, Banks L. Human papillomavirus type 16 E7 impairs the activation of the interferon regulatory factor-1. *Int J Mol Med* 2000; **5**: 661–6.
41 Antonsson A, Payne E, Hengst K, McMillan NA. The human papillomavirus type 16 E7 protein binds human interferon regulatory factor-9 via a novel PEST domain required for transformation. *J Interferon Cytokine Res* 2006; **26**: 455–61.

JOURNAL OF VIROLOGY, May 2009, p. 5137–5147 Vol. 83, No. 10
0022-538X/09/$08.00+0 doi:10.1128/JVI.02179-08

Involvement of Creatine Kinase B in Hepatitis C Virus Genome Replication through Interaction with the Viral NS4A Protein[▽]

Hiromichi Hara,[1,2] Hideki Aizaki,[1] Mami Matsuda,[1] Fumiko Shinkai-Ouchi,[3] Yasushi Inoue,[1,4] Kyoko Murakami,[1] Ikuo Shoji,[1,5] Hayato Kawakami,[6] Yoshiharu Matsuura,[7] Michael M. C. Lai,[8] Tatsuo Miyamura,[1] Takaji Wakita,[1] and Tetsuro Suzuki[1]*

Department of Virology II[1] and Department of Biochemistry and Cell Biology,[3] National Institute of Infectious Diseases, Tokyo 162-8640, Japan; Department of Internal medicine, Division of Pulmonary Diseases, The Jikei University School of Medicine, Tokyo 105-8461, Japan[2]; Mita Hospital, International University of Health and Welfare, Tokyo 108-8329, Japan[4]; Division of Microbiology, Kobe University Graduate School of Medicine, Hyogo 650-0017, Japan[5]; Department of Anatomy, Kyorin University School of Medicine, Tokyo 181-8611, Japan[6]; Research Institute for Microbial Diseases, Osaka University, Osaka 565-0871, Japan[7]; and Department of Molecular Microbiology and Immunology, University of Southern California, Keck School of Medicine, Los Angeles, California 90033[8]

Received 15 October 2008/Accepted 20 February 2009

Persistent infection with hepatitis C virus (HCV) is a major cause of chronic liver diseases. The aim of this study was to identify host cell factor(s) participating in the HCV replication complex (RC) and to clarify the regulatory mechanisms of viral genome replication dependent on the host-derived factor(s) identified. By comparative proteome analysis of RC-rich membrane fractions and subsequent gene silencing mediated by RNA interference, we identified several candidates for RC components involved in HCV replication. We found that one of these candidates, creatine kinase B (CKB), a key ATP-generating enzyme that regulates ATP in subcellular compartments of nonmuscle cells, is important for efficient replication of the HCV genome and propagation of infectious virus. CKB interacts with HCV NS4A protein and forms a complex with NS3-4A, which possesses multiple enzyme activities. CKB upregulates both NS3-4A-mediated unwinding of RNA and DNA in vitro and replicase activity in permeabilized HCV replicating cells. Our results support a model in which recruitment of CKB to the HCV RC compartment, which has high and fluctuating energy demands, through its interaction with NS4A is important for efficient replication of the viral genome. The CKB-NS4A association is a potential target for the development of a new type of antiviral therapeutic strategy.

Hepatitis C virus (HCV) infection represents a significant global healthcare burden, and current estimates suggest that a minimum of 3% of the world's population is chronically infected (4, 19). The virus is responsible for many cases of severe chronic liver diseases, including cirrhosis and hepatocellular carcinoma (4, 16, 19). HCV is a positive-stranded RNA virus belonging to the family *Flaviviridae*. Its ~9.6-kb genome is translated into a single polypeptide of about 3,000 amino acids (aa), in which the nonstructural (NS) proteins NS2, NS3, NS4A, NS4B, NS5A, and NS5B reside in the C-terminal half region (6, 34, 44). NS4A, a small 7-kDa protein, functions as a cofactor for NS3 to enhance NS3 enzyme activities such as serine protease and helicase activities. The hydrophobic N-terminal region of NS4A, which is predicted to form a transmembrane α-helix, is responsible for membrane anchorage of the NS3-4A complex (8, 44, 50), and the central region of NS4A is important for the interaction with NS3 (10, 44). A recent study demonstrated the involvement of the C terminus of NS4A in the regulation of NS5A hyperphosphorylation and viral replication (28).

The development of HCV replicon technology several years ago accelerated research on viral RNA replication (7, 44). Furthermore, a robust cell culture system for propagation of infectious HCV particles was developed using a viral genome of HCV genotype 2a, JFH-1 strain, enabling us to study every process in the viral life cycle (27, 47, 54). RNA derived from genotype 1a, HCV H77, containing cell-culture adaptive mutations, also produces infectious viruses (52). Using these systems, it has been reported that the HCV genome replicates in a distinct, subcellular replication complex (RC) compartment, which includes NS3-5B and the viral RNA (2, 14, 33). The RC forms in a distinct compartment with high concentrations of viral and cellular components located on detergent-resistant membrane (DRM) structures, possibly a lipid-raft structure (2, 41), which may protect the RC from external proteases and nucleases. Almost all processes in viral replication are dependent on the host cell's machinery and involve intimate interaction between viral and host proteins. However, the functional roles of host factors interacting with the HCV RC in viral genome replication remain ambiguous.

To gain a better understanding of cellular factors that are components of the HCV RC and that function as regulators of viral replication, a comparative proteomic analysis of DRM fractions from HCV replicon and parental cells and subsequent RNA interference (RNAi) silencing of selected genes were performed. We identified creatine kinase B (CKB) as a key factor for the HCV genome replication. CKB catalyzes the reversible transfer of the phosphate group of phosphocreatine

* Corresponding author. Mailing address: Department of Virology II, National Institute of Infectious Diseases, 1-23-1 Toyama, Shinjuku-ku, Tokyo 162-8640, Japan. Phone: 81-3-5285-1111. Fax: 81-3-5285-1161. E-mail: tesuzuki@nih.go.jp.

[▽] Published ahead of print on 4 March 2009.

(pCr) to ADP to yield ATP and creatine and is known to play important roles in local delivery and cellular compartmentalization of ATP (48, 51). The findings obtained here suggest that recruitment of CKB to the HCV RC, through CKB interaction with NS4A, is essential for maintenance or enhancement of viral replicase activity.

MATERIALS AND METHODS

Cell lines, antibodies, and reagents. Human hepatoma cell line Huh-7.5.1 (54) was kindly provided by Francis V. Chisari. Cell lines carrying subgenomic replicon RNAs, namely, SGR-N (41) and SGR-JFH1 (23), were derived from the HCV-N (17) and JFH-1 strains (24), respectively. Mouse monoclonal antibodies (MAbs) against HCV NS3 (Chemicon, Temecula, CA), NS4A (Santa Cruz Biotechnology, Inc., Santa Cruz, CA), NS5A (Biodesign, Saco, ME), NS5B (2), FLAG (M2; Sigma-Aldrich, St. Louis, MO), glyceraldehyde-3-phosphate dehydrogenase (GAPDH; Chemicon), and Flotillin-1 (BD Biosciences, San Jose, CA) and polyclonal antibodies (PAbs) against CKB (mouse [Abnova, Taipei, Taiwan], goat [Santa Cruz]), hemagglutinin (HA; Sigma-Aldrich), and FLAG (Sigma-Aldrich) were used. Cyclocreatine (Ccr; also known as 2-imino-1-imidazolidineacetic acid), pCr, and phosphopyruvic acid (pPy) were purchased from Sigma-Aldrich. Recombinant CKB and pyruvate kinase (PK) were obtained from Acris (Herfold, Germany) and Calbiochem (San Diego, CA), respectively.

Proteome analysis. RC-rich membrane fractions of cells were isolated as described previously (2, 41). Briefly, cells were lysed in hypotonic buffer. After removing the nuclei, supernatants were treated with 1% NP-40 for 60 min, mixed with 70% sucrose, overlaid with 55 and 10% sucrose, and centrifuged at 38,000 rpm for 14 h. Proteins from membrane fractions were purified by using a 2D Clean-Up kit (GE Healthcare, Tokyo, Japan), followed by labeling with fluorescent dyes: Cy5 for replicon cells, Cy3 for parental cells, and Cy2 for the protein standard containing equal amounts of both cell samples. Two-dimensional fluorescence difference gel electrophoresis (2D-DIGE) was performed using Immobiline DryStrip as the first-dimension gel and 12.5% polyacrylamide gel as the second-dimension gel. The 2D-DIGE images were analyzed quantitatively using the DeCyder software (GE Healthcare). Student *t* test was performed on differences between the tested samples using DeCyder biological variation analysis module. Samples were analyzed in triplicate. The protein spots of interest were excised from the gel, subjected to in-gel digestion using trypsin or lysyl endopeptidase and analyzed by liquid chromatography (MAGIC 2002 System; Michrom Bioresources, Auburn, CA) directly connected to electrospray ionization-ion trap mass spectrometry (LCQ-decaXP; Thermo Electron Corp., Iwakura, Japan). The results were subjected to database (NCBInr) search by Mascot server software (Matrix Science, Boston, MA) for peptide assignment.

Plasmids. A human CKB cDNA (43; kindly provided by Oriental Yeast Corp., Tokyo, Japan) was inserted into the EcoRI site of pCAGGS, yielding pCAGCKB. To generate expression plasmids for HA-tagged versions of wild-type and deletion mutated CKB, the corresponding DNA fragments were amplified by PCR, followed by introduction into the BglII site of pCAGGS. A fragment representing the inactive mutant CKB-C283S was synthesized by PCR mutagenesis. To generate FLAG-tagged NS protein expression plasmids, DNA fragments encoding either NS3, NS4A, NS4B, NS5A, or NS5B protein were amplified from HCV strains NIHJ1 (1) and JFH-1 (23) by PCR, followed by cloning into the EcoRI-EcoRV sites of pcDNA3-MEF (20). To generate an HA-tagged NS3 expression plasmid, a fragment encoding NS3 with the HA tag sequence at its N terminus was inserted into pCAGGS.

siRNA transfection. The small interfering RNAs (siRNAs) targeted to CKB (CKB-1 [5′-UAAGACCUUCCUGGUGUGGTT-3′] and CKB-2 [5′-CGUCACCCUUGGUAGAGUUTT-3′]) and the scramble negative control siRNA to CKB-2 (5′-GGCGUACUAGCUUAUUCGCTT-3′) were purchased from Sigma. Cells in a 24-well plate were transfected with siRNA using HiPerFect transfection reagent (Qiagen, Tokyo, Japan) according to the manufacturer's instructions. The siRNA sequences for the other genes used in the siRNA screening are available upon request.

HCV infection. Culture media from Huh-7 cells transfected with in vitro-transcribed RNA corresponding to the full-length JFH-1 (47) was collected, concentrated, and used for the infection assay (3).

Quantification of HCV core protein and RNA. To estimate the levels of HCV core protein, aliquots of culture supernatants or of cell lysates were assayed by using HCV Core enzyme-linked immunosorbent assay kits (5). Total RNA was isolated from harvested cells using TRIzol (Invitrogen, Carlsbad, CA). Copy numbers of the viral RNA were determined by reverse transcription-PCR (RT-PCR) (2, 36, 46).

Immunoprecipitation, immunoblot analysis, and immunofluorescence microscopy. The analyses, as well as DNA transfection, were performed essentially as previously described (42). Cells were lysed in immunoprecipitation lysis buffer (50 mM Tris-HCl [pH 7.6], 150 mM NaCl, 1% sodium deoxycholate, 1% NP-40, 0.1% sodium dodecyl sulfate, 1 mM dithiothreitol, 1 mM calcium acetate). For immunoprecipitation, supernatants of cell lysates were precipitated with anti-FLAG antibody and protein A-Sepharose Fast Flow beads (GE healthcare). For immunofluorescence microscopy, anti-CKB goat PAb and anti-NS4A MAb as primary antibodies and Alexa Fluor 555-conjugated donkey anti-goat immunoglobulin G (Invitrogen) and Alexa Fluor 488-conjugated rabbit anti-mouse immunoglobulin G (Invitrogen) as secondary antibodies were used and observed under an LSM 510 confocal microscope (Carl Zeiss, Oberkochen, Germany).

Immunoelectron microscopy. Postembedding immunostaining using the colloidal gold-labeling method was performed as described previously (38). Cells were fixed in 4% paraformaldehyde–1% glutaraldehyde at 4°C for 1 h. After dehydration through a graded series of ethanol, cells were embedded in LR White (London Resin Company, London, United Kingdom) and sectioned. After blocking, section grids were incubated with a mixture of anti-NS4A and anti-CKB antibodies at 4°C overnight, followed by treatment with a mixture of 18-nm colloidal gold-conjugated donkey anti-mouse immunoglobulin G and 12-nm colloidal gold-conjugated donkey anti-goat immunoglobulin G antibodies (Jackson Immunoresearch, West Grove, PA) at 4°C overnight. The sections were stained with uranyl acetate and observed under a transmission electron microscope.

Measurement of CK activity and cellular ATP level. Cells were lysed with passive lysis buffer (Promega, Madison, WI), and CK activities were measured based on Oliver methods (40), in which the activity of converting creatine phosphate and ADP to creatine and ATP was measured. ATP levels in cell lysates were measured by using a CellTiter-Glo luminescent cell viability assay (Promega).

RNA replication assays in permeabilized replicon cells and in vitro. The RNA synthesis assay using permeabilized replicon cells was based on a previously described method (33). Briefly, SGR-JFH1 cells were treated with 5 μg of actinomycin D/ml for 2 h, followed by permeabilization with 50 μg of digitonin/ml for 5 min. The resulting mix was incubated with 500 μM concentrations of ATP, GTP, and CTP; 10 μCi of UTP ([α-^{32}P]UTP); 50 μg of actinomycin D/ml; and 5 mM pCr with or without 20 U of CKB/ml for 4 h at 27°C. RNA was extracted by using TRIzol and analyzed by 1% formaldehyde agarose gel electrophoresis. The cell-free RNA replication assay was performed as described previously (2).

In vitro helicase assays. Helicase activity on double-stranded RNA (dsRNA) was investigated as described previously (11) with some modifications. The 5′ end of the release strand was labeled with [γ-^{32}P]ATP using T4 polynucleotide kinase (Ambion). The dsRNA substrate was obtained by annealing the labeled RNA with a template strand RNA at a molar ratio of 1:1. The helicase assay mixture contained 5 nM dsRNA, helicase enzyme (80 nM NS3 or NS3-4A [kindly provided by R. De Francesco]), 6 mM ATP, in the presence or absence of 20 U of CKB/ml in an assay buffer (25 mM MOPS-NaOH [pH 7.0], 2.5 mM dithiothreitol, 100 μg of bovine serum albumin/ml, 3 mM $MgCl_2$, 5 mM pCr, 2.5 U of RNase inhibitor/ml). After the helicase reaction, samples were electrophoresed in a native 8% polyacrylamide gel and autoradiographed.

To determine the effect of PK/pPy system on the helicase activity, PK and pPy were used instead of CKB and pCr. Helicase activity on dsDNA was measured based on homogeneous time-resolved fluorescence quenching using a Trupoint helicase assay kit (Perkin-Elmer, Waltham, MA) according to the manufacturer's instructions.

In vitro protease assay. In vitro HCV protease activity of NS3-4A or NS3 was analyzed by using a SensoLyteHCV protease assay kit (AnaSpec, San Jose, CA) according to the manufacturer's instructions.

RESULTS

Identification of host factors involved in HCV RNA replication by comparative proteomic analysis of DRM fractions and RNAi silencing. To identify host proteins involved in the HCV RC, proteome profiles of the RC-rich membrane fraction in Huh-7 cells harboring subgenomic replicon RNA derived from genotype 1b, N isolate (SGR-N) were compared to those of parental cells by 2D-DIGE. We confirmed that the DRM fraction obtained from SGR-N cells is functionally active in a

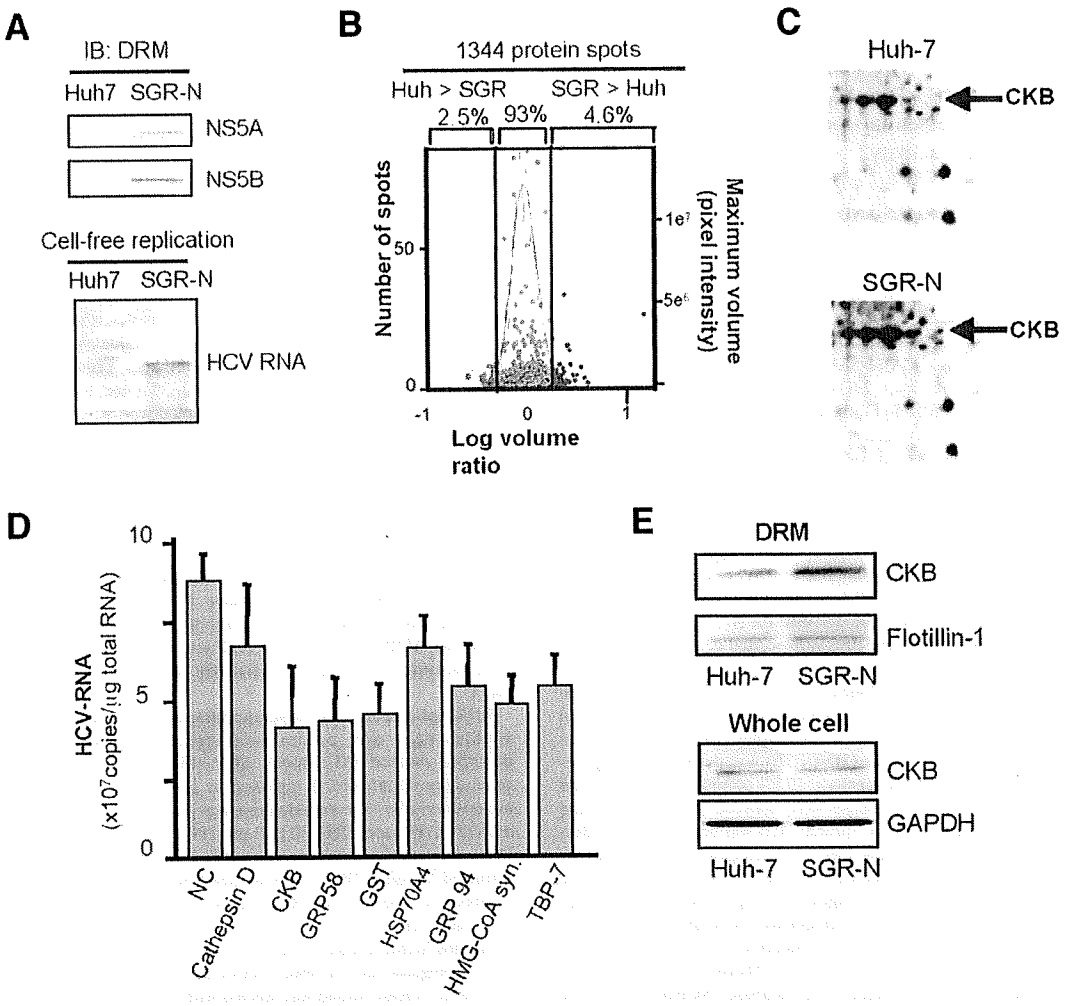

FIG. 1. Comparative proteomic analysis of DRM fractions and RNAi silencing. (A) Preparation of functionally active RC fraction for proteome analysis. DRM fractions obtained from SGR-N cells and parental Huh-7 cells were analyzed by immunoblotting with anti-NS5A and anti-NS5B antibodies (upper panel) and by the cell-free RNA replication assay (lower panel). (B) Histogram representation of proteins detected in 2D-DIGE. Images were analyzed quantitatively by the DeCyder software. The left and right *y* axis, respectively, indicate the spot frequency and the maximum volume of each spot, given against the log volume ratio (*x* axis). (C) Comparison of 2D-DIGE maps of proteins from DRM fractions of SGR-N cells and Huh-7 cells. Enlarged 2D-DIGE gel images of regions containing protein spots of CKB (arrows) are shown. (D) Effects of siRNAs of genes selected from comparative proteome analysis on HCV RNA replication. SGR-N cells were transfected with siRNA specific to cathepsin D, CKB (siCKB-1), GRP58, GST, Hsp70 protein 4, GRP94, HMG-coenzyme A synthase, or Tat binding protein 7 or with nontargeting (NC) siRNA. At 48 h posttransfection, total RNA was isolated and HCV RNA levels were assessed by real-time RT-PCR. (E) Enrichment of CKB in the DRM of HCV replicon cells. Equal amounts of DRM fractions from SGR-N and parental Huh-7 cells, or whole-cell lysates from both cells were analyzed by immunoblotting with antibodies against CKB, flotilin-1 or GAPDH.

cell-free replication assay (Fig. 1A). Three independent proteome experiments were performed for a reliable analysis of protein expression. Approximately 1,300 spots were resolved in each gel, and 4 to 5% of the protein spots represented a >2-fold increase in the membrane fraction of replicon cells in each experiment (Fig. 1B). The protein spots that exhibited high reproducibility (an example shown in Fig. 1C) were excised, digested by trypsin or lysyl endopeptidase, and analyzed by mass spectrometry, which identified the corresponding proteins in 27 cases (Table 1). Among the proteins implicated in a variety of functional categories, 10 were involved in protein folding, mainly as chaperones, 7 were metabolic and biosynthesis enzymes including proteins for redox regulation or energy pathways, 3 were involved in cytoskeleton organization, and 3 proteins were related to cellular processes, mainly proteolysis pathways. The viral NS proteins identified as differentially expressed proteins in the analysis were not listed.

In order to identify host factors involved in HCV replication, we examined the effects on viral RNA replication of transfection of SGR-N cells with siRNAs against genes encoding nine proteins belonging to diverse classes of biological functions (Table 1). Each siRNA reduced the HCV RNA level to 47 to 76% of the level of the siRNA control (Fig. 1D). None of the siRNAs tested exhibited considerable cytotoxicity against the replicon cells, ruling out overt toxicity as a mechanism for inhibition of viral RNA replication. Among the candidate

TABLE 1. Selected proteins that reproducibly increased in the DRM fraction of SGR-N cells[a]

Avg ratio	*P* (Student *t* test)	Coverage (%)	Protein name	Molecular function	GI no.
5.56	0.04	27	GRP94	Protein folding	15010550
4.99	0.07	47	Hsp60	Protein folding	6996447
3.73	0.07	6	tRNA guanine transglycosylase	Metabolism	30583205
3.56	0.06	23	KIAA0088	Unknown	577295
3.32	0.07	4	Thioredoxin-related protein	Unknown	20067392
3.32	0.13	12	Tat binding protein 1 (TBP-1)	Cellular processes	20532406
3.06	0.14	22	Aldehyde dehydrogenase 1	Metabolism	2183299
3.06	0.14	14	Chaperonin TRiC/CCT, subunit 2	Protein folding	54696794
2.96	0.04	14	Heat shock 70-kDa protein 4 (HSPA4)	Protein folding	6226869
2.96	0.04	29	GRP58	Metabolism/protein folding	2245365
2.94	0.01	37	Mutant β-actin	Cytoskeleton organization	28336
2.65	0.17	33	Glutathione S-transferase (GST)	Catalytic activity	2204207
2.53	0.04	37	Keratin 19	Cytoskeleton organization	6729681
2.46	0.08	6	Heterogeneous nuclear ribonucleoprotein K	Nucleic acid modification	460789
2.45	0.001	13	HMG-coenzyme A synthase	Metabolism	30009
2.4	0.02	31	CKB	Energy pathway/metabolism	180570
2.4	0.02	11	Cathepsin D	Cellular processes	30582659
2.4	0.02	11	C8orf2	Unknown	37181322
2.36	0.1	38	Tropomyosin 4-anaplastic lymphoma kinase fusion protein	Cytoskeleton organization	14010354
2.36	0.1	6	Calreticulin	Protein folding	30583735
2.33	0.01	29	Quinolinate phosphoribosyltransferase	Metabolism	30583301
2.29	0.04	25	Protein disulfide isomerase-related protein 5	Protein folding	1710248
2.29	0.04	16	Tat binding protein 7 (TBP-7)	Cellular processes	263099
2.05	0.11	24	Calumenin	Metabolism	2809324
2.05	0.12	10	TRiC/CCT, subunit 5	Protein folding	24307939
2.03	0.07	20	Hsp90 beta	Protein folding	34304590
2.01	0.07	10	TRiC/CCT, subunit 1	Protein folding	36796

[a] The spectra obtained by tandem mass spectrometry were collected using data-dependent mode, and the results were subjected to database (NCBInr) search by Mascot server software (Matrix Science, London, United Kingdom) for peptide assignment. Coverage, the ratio of the portion of protein sequence covered by matched peptides to the whole protein sequence. GI no., GenInfo identifier number.

genes examined, we observed a reproducible inhibition of HCV RNA replication by two independent siRNAs targeting CKB (see below).

CKB participates in HCV RNA replication and the propagation of infectious virus. CKB is a brain-type creatine kinase isoenzyme and is also detected in a variety of other tissues, including human liver (32). Steady-state levels of CKB in the DRM fraction, as well as in whole-cell lysate of SGR-N cells were compared to those from parental cells by Western blotting. The CKB level in the DRM fraction of replicon cells was higher than that in parental cells (Fig. 1E), confirming the results of the proteome analysis described above. In contrast, the CKB level in whole cells was similar in both cells (Fig. 1E). These results suggest participation of posttranslational modification, such as translocation to the DRM fraction, of CKB in replicon cells.

Figure 2A shows the inhibitory effect on HCV RNA replication of CKB siRNA; siCKB-2, the sequence of which does not overlap with the sequence of siCKB-1 used in the above siRNA screening (Fig. 1D). Transfection with siCKB-2 effectively decreased the cellular level of CKB enzymatic activity (data not shown), as well as the abundance of CKB protein (Fig. 2A), and resulted in 60% reduction in the viral RNA level in SGR-N cells compared to the cells treated with control siRNA. This inhibitory effect of siRNA on HCV RNA abundance was also observed in JFH-1-derived subgenomic replicon (SGR-JFH1) cells. The viral RNA level in the cells transfected with siCKB-2 decreased by 50% compared to the control (Fig. 2A). We also tested the CKB mutant, CKB-C283S, in which Cys at aa 283, near the catalytic site, has been replaced with Ser (Fig. 3A) and which is known to be enzymatically inactive and to work in a dominant-negative manner (22, 29). As expected, overexpression of CKB-C283S resulted in a reduction in HCV RNA replication in SGR-N cells (Fig. 2B). We obtained a similar result in SGR-JFH1 cells, as described below (Fig. 3E).

To further examine the involvement of CKB in HCV RNA replication, we tested the effect of Ccr, a substrate analogue and possible inhibitor for CK in either SGR-N, SGR-JFH1 (Fig. 2C), or Huh7 cells transiently replicating luciferase-subgenomic replicon (data not shown). We found dose-dependent inhibition of HCV RNA replication but no observed effect on total cellular levels of protein and ATP (Fig. 2D) in the replicon setting used.

We next examined whether the knockdown of CKB or treatment with Ccr would abrogate the production of HCVcc. At 72 h posttransfection with siCKB-2, the HCV core level in cells infected with HCVcc was significantly reduced (Fig. 2E). Treatment of the infected cells with Ccr at various concentrations also reduced the intracellular and supernatant core level and subsequently decreased HCVcc production (Fig. 2F). These results demonstrate that suppression of the HCV RNA replication by the siRNA-mediated knockdown of CKB or treatment with CKB inhibitor leads to reduction of the production of infectious virus.

CKB interacts with HCV NS4A. Having established a role for CKB in HCV RNA replication, we then tried to determine to how CKB influences the HCV life cycle. It has been re-

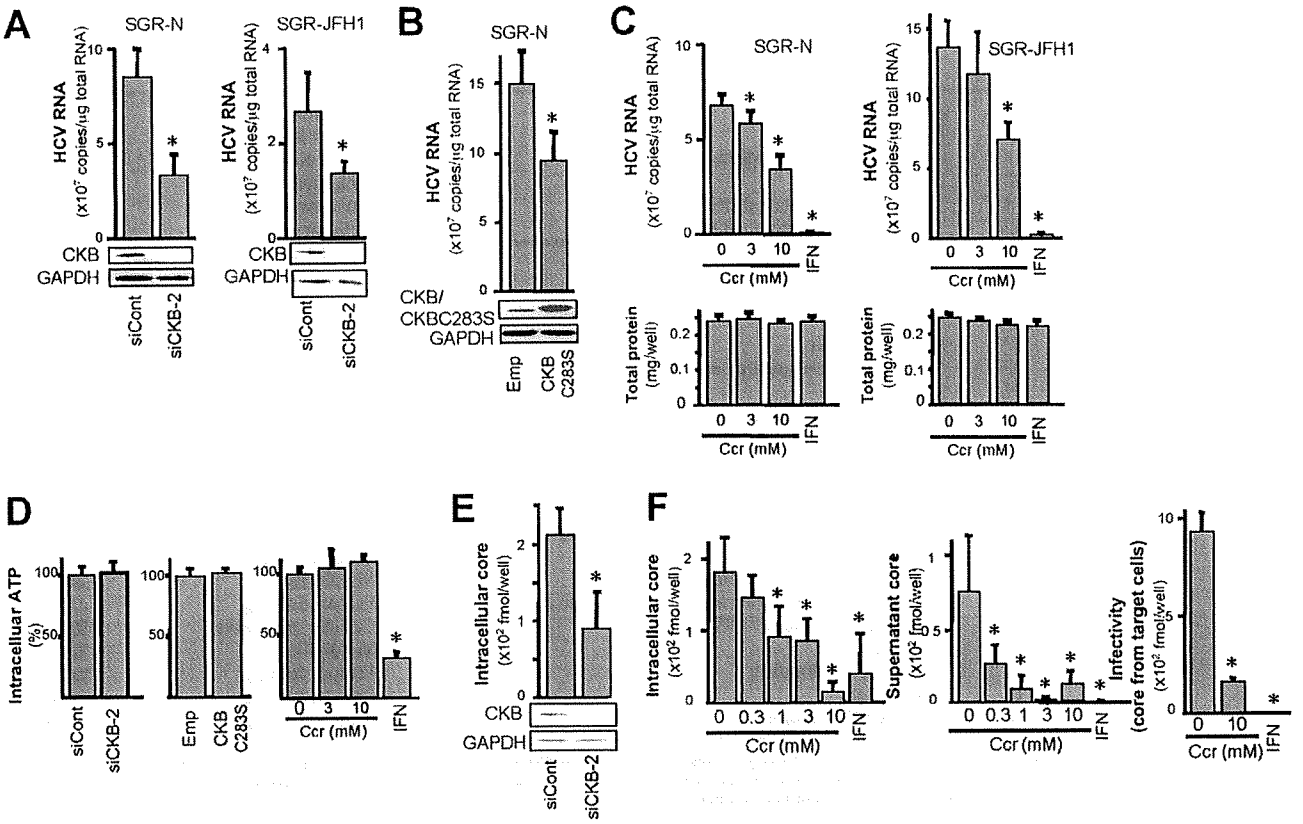

FIG. 2. Involvement of CKB in HCV replication. (A and E) Knockdown of endogenous CKB in SGR-N and SGR-JFH1 cells (A) or HCVcc-infected cells (E). Cells were transfected with siRNA against CKB (siCKB-2) or control siRNA (siCont) and were harvested at 72 h posttransfection. Real-time RT-PCR for HCV RNA levels and immunoblotting for CKB and GAPDH were performed. (B) SGR-N cells were transfected with pCAGCKB-C283S or empty vector, and HCV RNA levels and expression of CKB and CKB-C283S were determined 72 h posttransfection. SGR-N and SGR-JFH1 cells (C) or HCVcc-infected cells (F) were treated with Ccr at various concentrations for 72 h, followed by quantification of HCV RNAs and total cellular proteins. ATP levels (D) were determined after transfection with siCKB-2, pCAGCKB-C283S, or treatment with Ccr for 72 h in SGR-N cells. The ATP levels in the cells transfected with negative control siRNA (left), empty vector (middle), and no treatment (right) were set at 100%, respectively. (F) HCVcc-infected cells were treated with Ccr, and the viral core protein levels in cells (left) and supernatants (middle) were determined at 72 h postinfection. Collected culture supernatants were inoculated into naive Huh-7.5.1 cells after the removal of Ccr. After 72 h, the core proteins in cells were determined (right panel). All data are presented as averages and standard deviation values for at least triplicate samples. *, $P < 0.05$ against control such as transfection with siCont (A and E) or empty vector (B) or nontreatment (C, D, and F).

ported that interaction of CKB with some cellular proteins is required for local availability of CKB activity and local generation of ATP (22, 29). To examine the possible interaction of CKB with HCV NS proteins, HA-tagged CKB (HA-CKB) was coexpressed with FLAG-tagged NS proteins (NIHJ1 strain), followed by immunoprecipitation with an anti-FLAG antibody. CKB was shown to specifically interact with NS4A. No or little interaction was observed between CKB and either NS3, NS4B, NS5A, or NS5B (Fig. 3B). CKB-NS4A interaction was also found with the JFH-1 strain (Fig. 3C).

To identify the CKB region required for the interaction with NS4A, various deletion mutants of CKB were generated (Fig. 3A). An immunoprecipitation assay indicated that NS4A was coimmunoprecipitated with either a full-length CKB, a C-terminal deletion (aa 1 to 357), an N-terminal deletion (aa 297 to 381), or CKB-C283S, but not with aa 1 to 296, aa 1 to 247, or aa 1 to 184 (Fig. 3D, upper middle panel). Further, internal deletions of CKB (CKBdel297-357 and CKB-C283Sdel297-357) failed to interact with NS4A (Fig. 3D, lower panel), suggesting that aa 297 to 357 of CKB are important for its interaction with NS4A. It is noted that the expression of CKB aa 297 to 357 in cells was undetected, presumably due to its misfolding and/or instability. To verify a role for CKB-NS4A interaction in HCV RNA replication, we further determined the effect of expression of either CKB-C283S or its internal deletion lacking aa 297 to 357 (CKB-C283Sdel297-357) on viral replication in SGR-JFH1 cells. As expected, the HCV RNA level was significantly decreased by CKB-C283S, whereas this effect was not observed by CKB-C283Sdel297-357 (Fig. 3E).

NS4A is a 54-residue small protein composed of three domains: the N-terminal membrane anchor, the central domain responsible for interacting with NS3, and the C-terminal acidic domain. To define the portion in NS4A responsible for its interaction with CKB, we constructed three NS4A deletion mutants, each separately expressing one of the NS4A domains, with a FLAG tag (Fig. 3F). CKB proved to interact with the central domain, aa 21 to 39, of NS4A, which is involved in

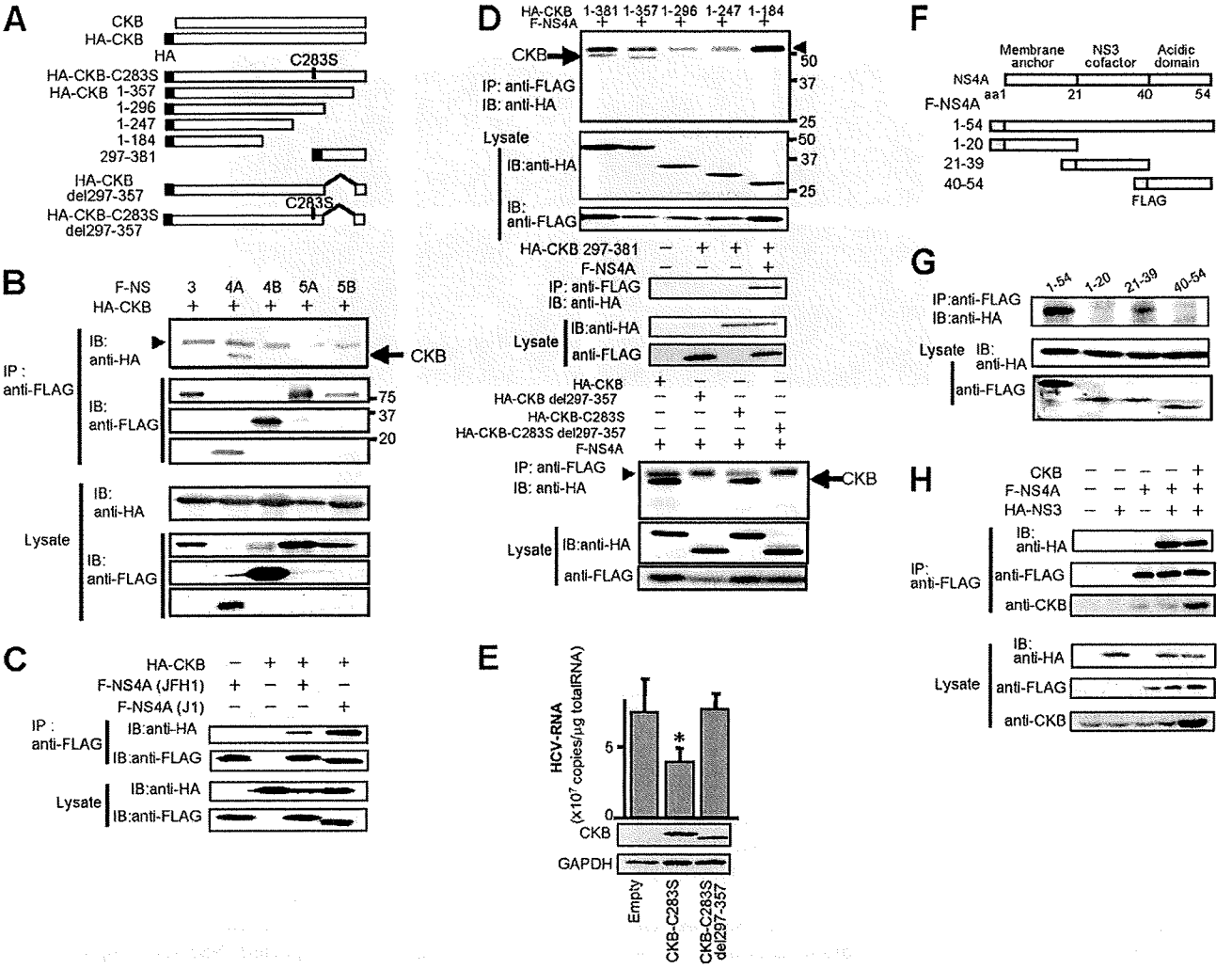

FIG. 3. CKB interacts with HCV NS4A. (A) Structures of CKB constructs used in the present study. A full-length wild-type CKB without an epitope tag (CKB) or with an N-terminal HA tag (HA-CKB), HA-CKB with deletions (aa 1 to 357, aa 1 to 296, aa 1 to 247, aa 1 to 184, and aa 297 to 381 and del297-357), CKB mutant at the catalytic site, Cys-283 (CKB-C283S) or CKB-C283S lacking aa 297 to 357 (CKB-C283Sdel297-357) are shown. HA-CKB was coexpressed with FLAG-tagged versions of each NS protein of strain NIHJ1 (B) or with NS4A of strain JFH-1 (C) in 293T cells and immunoprecipitated (IP) with an anti-FLAG antibody. Immunoprecipitates were subjected to immunoblotting (IB) with anti-HA or anti-FLAG antibody. (D) Each CKB deletion mutant was coexpressed with FLAG-NS4A in 293T cells. Immunoprecipitates were analyzed by immunoblotting. Arrow, CKB; arrowhead, immunoglobulin heavy chain. (E) SGR-JFH1 cells were transfected with the expression plasmid for CKB-C283S, CKB-C283Sdel297-357 or empty vector. At 72 h posttransfection, HCV RNA levels and the expression of CKB and CKB-C283S were determined by real-time RT-PCR and immunoblotting with anti-HA antibody, respectively. For HCV RNA quantitation, data are indicated as averages and standard deviations ($n = 3$). *, $P < 0.05$ against the empty vector control. (F) Structure of NS4A and NS4A constructs. FLAG-tagged NS4A (aa 1 to 54) or its truncated mutants (aa 1 to 20, aa 21 to 39, or aa 40 to 54) are shown. (G) Each NS4A deletion mutant was coexpressed with HA-CKB and analyzed as described above. (H) FLAG-NS4A was coexpressed with HA-NS3 or HA-NS3 and CKB, followed by immunoprecipitation with anti-FLAG antibody. Immunoprecipitates were analyzed by immunoblotting with anti-HA, anti-FLAG or anti-CKB antibody.

formation of the NS3-NS4A complex (Fig. 3G). We therefore investigate whether NS3-NS4A interaction is affected in the presence of CKB and found that exogenous expression of CKB has no influence on NS3-NS4A interaction, and a putative NS3-NS4A-CKB complex was detected in the coimmunoprecipitation analysis (Fig. 3H). Collectively, these results strongly suggest that CKB plays a key role in HCV RNA replication via interaction with NS4A.

Subcellular localization of CKB and NS4A in cells replicating HCV RNA. CKB is distributed throughout cells but is mainly localized in the perinuclear area (31), whereas NS4A is predominantly localized at the endoplasmic reticulum and mitochondrial membranes (37). We examined the possible subcellular colocalization of CKB and NS4A in SGR-N cells by immunofluorescence staining (Fig. 4A). CKB tended to gather in the perinuclear area of HCV replicating cells and was partially colocalized with NS4A in the area, sharing a dotlike structure. To further analyze the subcellular compartments in which CKB and NS4A coexist, we used double-labeling immunoelectron microscopy on SGR-N cells using antibodies against CKB and NS4A, with secondary antibodies coupled to 12- and 18-nm gold particles, respectively. One fraction of

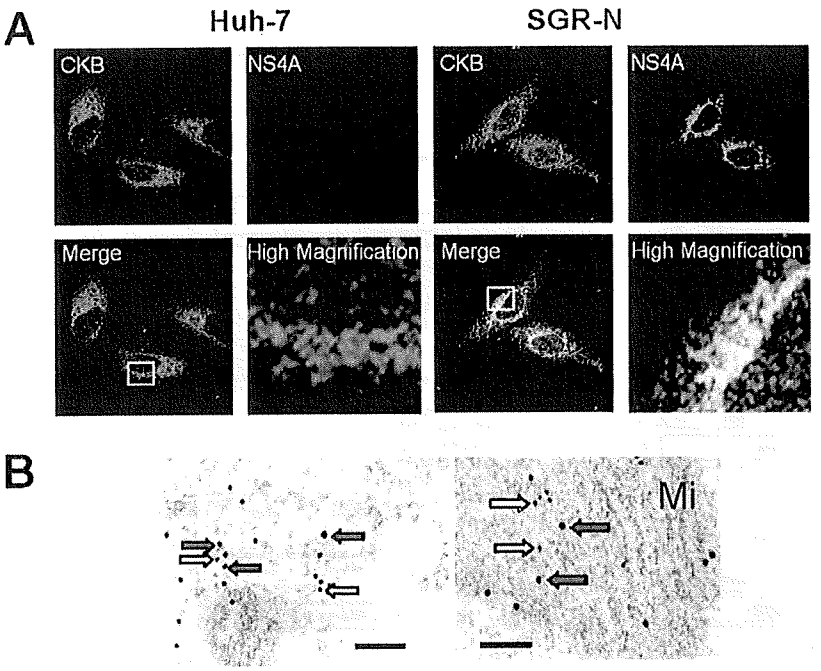

FIG. 4. Colocalization of CKB with HCV NS4A. (A) Indirect immunofluorescence analysis. The primary antibodies used were anti-CKB goat PAb (red) and anti-NS4A MAb (green). Merged images of red and green signals are shown. High-magnification panels are enlarged images of white squares in the merge panels. (B) Immunoelectron microscopic localization of CKB and NS4A. SGR-N cells were double-immunolabeled for CKB (12-nm gold particles; white arrows) and for NS4A (18-nm gold particle; gray arrows). Mi, mitochondria. Bars, 200 nm.

CKB colocalized with NS4A in the cytoplasmic electron-dense regions, presumably derived from altered or folded membrane structures (Fig. 4B, left panel) and mitochondria (Fig. 4B, right panel).

CKB enhances functional HCV replicase and NS3-4A helicase. NS4A is known to mediate membrane association of the NS3-4A complex and to function as a cofactor in NS3 enzyme activity. To understand the mechanism(s) underlying positive regulation of HCV RNA replication through CKB via its interaction with NS4A, we first investigated whether CKB modulates NS3-4A helicase activity. NS3-4A helicase is a member of the superfamily-2 DexH/D-box helicase, which unwinds RNA-RNA substrates in a 3′-to-5′ direction. During RNA replication, the NS3-4A helicase is believed to translocate along the nucleic acid substrate by changing its protein conformation, utilizing the energy of ATP hydrolysis (9). We then tested the effect of CKB on RNA- or DNA-unwinding activity using purified recombinant full-length NS3 and NS3-4A complex (12). As shown in Fig. 5A (left middle panel), both NS3 and NS3-4A helicase activity unwound dsRNA substrate most efficiently when CKB, ATP, and pCr were added to the reaction mixture. The enhancing effect of CKB was observed in the presence of pCr but not in the absence of it, suggesting that catalytic activity of CKB is important for its effect on the HCV helicase activity. Similar results were obtained from the DNA helicase assay using dsDNA substrate (Fig. 5B). To address the specificity of the stimulation by the CKB/pCr system, effects of PK and pPy, which are also involved in the ATP generation, were determined (Fig. 5A, right panels). Exogenous PK and pPy at the same concentrations as those of CKB and pCr used in the study exhibited no effect on the HCV helicase activity.

The effect of CKB on NS3-4A serine protease activity, which is considered to be ATP-independent, was also assessed in an in vitro protease assay using the purified viral proteins as mentioned above (Fig. 5C). As expected, NS3-4A complex exhibited significantly higher activity than NS3 alone; however, CKB did not affect the protease activities of NS3 or NS3-4A.

Finally, we investigated loss and gain of function of CKB in HCV replicase activity, which requires high-energy phosphate, in the context of semi-intact replicon cells. Miyanari et al. (33) reported that the function of the active HCV RC can be monitored in permeabilized replicon cells treated with digitonin. Thus, permeabilized replicon cells in the presence or absence of exogenous CKB were incubated with [α-^{32}P]UTP to detect newly synthesized RNA. As indicated in Fig. 5D, an ~8-kb band corresponding to HCV subgenomic RNA was most abundant in cells in the presence of exogenous CKB, ATP and pCr. The enhancing effect of CKB was observed in the presence but not in the absence of pCr, suggesting that catalytic activity of CKB is important for its effect on the replicase activity. As for the RNA helicase assay, exogenous PK and pPy did not enhance the replicase activity (data not shown). HCV replicase activity in permeabilized cells to which we had introduced siCKB-2 was diminished compared to that in siRNA control-treated cells. Interestingly, the replicase activity in the CKB-depleted cells was recovered by the addition of CKB. Thus, our findings suggest that CKB functions as a key regulator of HCV genome replication by controlling energy-dependent viral enzyme activities.

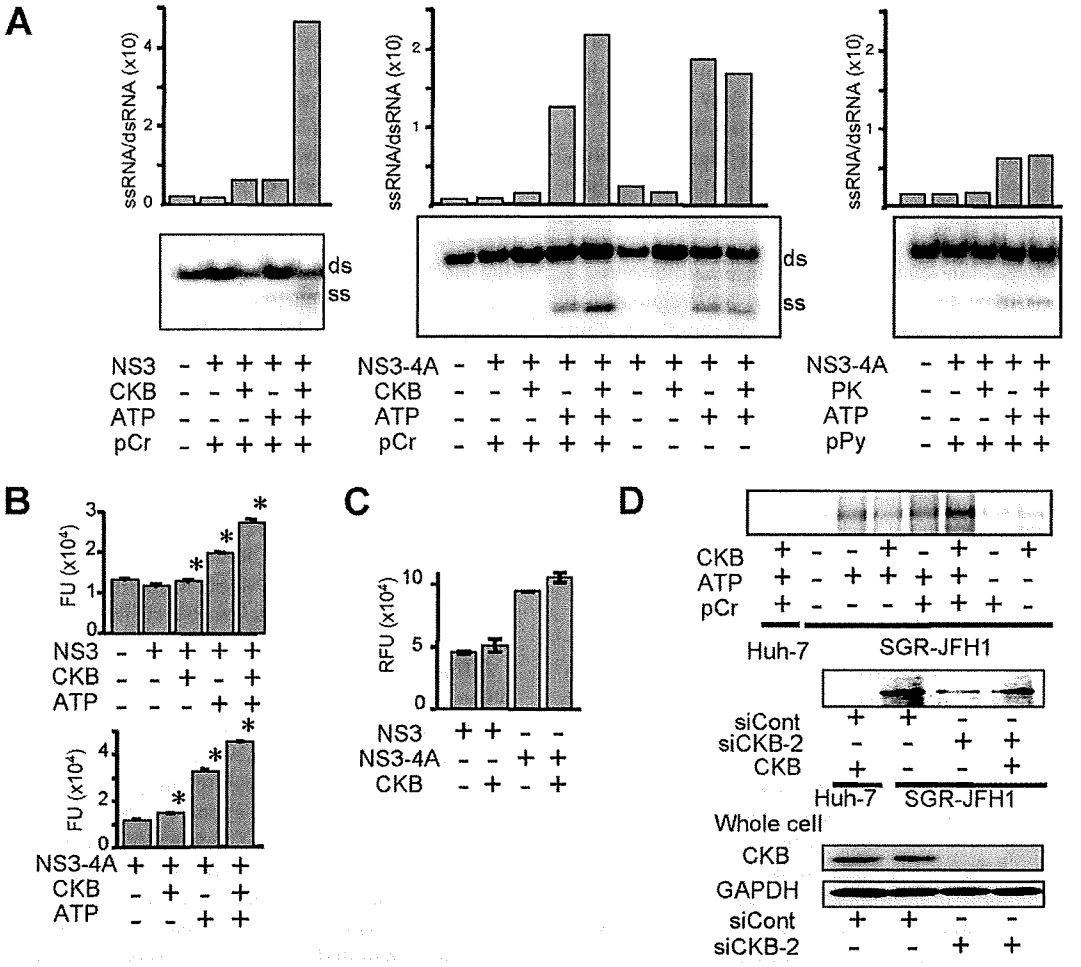

FIG. 5. CKB enhances NS3-4A helicase and HCV replicase activities. (A) In vitro RNA helicase activity of NS3-4A or NS3 was determined by detecting unwound single-strand RNA (ss) derived from the partially dsRNA substrate (ds). Band intensities corresponding to unwound products and those to dsRNA substrates were determined by ImageQuant 5.2 (Molecular Dynamics), and the ssRNA/dsRNA ratios were calculated. The results are representative of three similar experiments. (B) In vitro DNA helicase activity of NS3-4A or NS3 was analyzed by using a commercially available kit. The data represent averages and standard deviations ($n = 3$). *, $P < 0.05$ against the value without supplementation of CKB and ATP. (C) The in vitro HCV protease activity of NS3-4A or NS3 in the presence or absence of CKB was analyzed. Error bars represent standard deviations ($n = 3$). (D) Replicase activity in permeabilized replicon cells. The upper panel shows the activity for synthesis of HCV subgenomic RNA in the digitonin-permeabilized SGR-JFH1 cells with or without supplementation of CKB was measured. The middle panel shows results for SGR-JFH1 or Huh-7 cells that were transfected with siCKB-2 or siCont and permeabilized at 72 h posttransfection. The permeabilized cells with or without supplementation of CKB were subjected to the replicase assay. The lower panel shows the immunoblotting results for whole-cell lysates of siRNA-transfected cells.

DISCUSSION

Viral replication requires energy and macromolecule synthesis, and host cells provide the viruses with metabolic resources necessary for their efficient replication. Thus, it is highly likely that interaction of viruses with host cell metabolic pathways, including energy-generating systems, contributes to the virus growth cycle. In the regulation of HCV genome replication, the functions of the viral NS proteins that comprise the RC might be regulated by association in individual host cell factors. For example, hVAP-A and -B function as cofactors of modulating RC formation via interacting with NS5A and NS5B (13, 18). Cyclophilin B is involved in stimulating viral RNA binding activity via interacting with NS5B (49). FKBP8 (39) and hB-ind1 (45) play an important role in recruiting Hsp90 to RC via interacting with NS5A. However, the association of viral protein(s) with the cellular energy-generating system to directly regulate the activity of the RC has not been well understood.

In the present study, the accumulation of CKB, an ATP-generating enzyme, in the HCV RC-rich membrane fraction of viral replicating cells and its importance in replication of the HCV genome and production of infectious virions have been demonstrated. Enzymatic analyses with semi-intact replicon cells and purified NS3-4A protein revealed that CKB enhances the functional replicase and helicase of HCV. Its enhancing effect was observed in the presence of pCr but not in its absence, suggesting that the catalytic activity of CKB is important for enhancing the replicase and